ETD Archive

2018

High-throughput Metabolism-induced Toxicity Assays on a 384-pillar Plate

Sooyeion Kang
Cleveland State University

HIGH-THROUGHPUT METABOLISM-INDUCED TOXICITY ASSAYS

ON A 384-PILLAR PLATE

SOO-YEON KANG

Bachelor of Chemical and Biological Engineering

Gachon University

February 2016

Submitted in partial fulfillment of requirements for the degree

MASTER OF SCIENCE IN CHEMICAL ENGINEERING

at

CLEVELAND STATE UNIVERSITY

August 2018

We hereby approve the thesis for

SOOYEON KANG

Candidate for the Master of Science in Chemical Engineering degree for the

Department of Chemical and Biomedical Engineering

and CLEVELAND STATE UNIVERSITY'S

College of Graduate Studies by

_____

Thesis Chairperson, Dr. Moo-Yeal Lee
Chemical and Biomedical Engineering Department

_____

Date

_____

Thesis Committee Member, Dr. Chandrasekhar R. Kothapalli
Chemical and Biomedical Engineering Department

_____

Date

_____

Thesis Committee Member, Dr. Geyou Ao
Chemical and Biomedical Engineering Department

_____

Date

Date of Defense: April 27, 2018

ACKNOWLEDGMENTS

I would like to express my deep appreciation and indebtedness to countless individuals. First, I would like to mention my family. Being away from them is a toughest part but they are the ones who keep on encouraging me whenever I get knocked down.

I would like to thank my research advisor, Dr. Moo-Yeal Lee, for the support and guidance that he provided me throughout my experience at Cleveland State University. I am grateful to my thesis committee members, Dr. Chandrasekhar R. Kothapalli and Dr. Geyou Ao for the comments and encouragement.

I want to thank all my lab mates for their immense help, love and support. Special thanks to Dr. Kyeong-Nam Yu, Pranav Joshi, and Stephen Hong for all the moral support, inspiration and motivation. Their participation and assistance made the completion of this thesis possible.

HIGH-THROUGHPUT METABOLISM-INDUCED TOXICITY ASSAYS
ON A 384-PILLAR PLATE

SOO-YEON KANG

ABSTRACT

The U.S Environmental Protection Agency (EPA) launched the Transform Tox Testing Challenge in 2016 with the goal of developing practical methods that can be integrated into conventional high-throughput screening (HTS) assays to better predict the toxicity of parent compounds and their metabolites *in vivo*. In response to this need and to retrofit existing HTS assays for assessing metabolism-induced toxicity of compounds, we have developed a 384-pillar plate that is complementary to traditional 384-well plates and ideally suited for culturing human cells in three dimensions (3D) at a microscale. Briefly, human embryonic kidney (HEK) 293 cells in a mixture of alginate and Matrigel were printed on the 384-pillar plates using a microarray spotter. These cells were then coupled with 384-well plates containing nine model compounds provided by the EPA, five representative Phase I and II drug metabolizing enzymes (DMEs), and one no enzyme control. Membrane integrity and viability of HEK 293 cells were measured with the calcein AM and CellTiter-Glo® kit, respectively, to determine the IC_{50} values of the nine parent compounds and DME-generated metabolites. Out of the nine compounds tested, six compounds showed augmented toxicity with DMEs and one compound showed detoxification with a Phase II DME. This result indicates that the 384-pillar plate platform can be used to measure metabolism-induced toxicity of compounds with high predictivity. In addition, the Z' factors and the coefficient of variation (CV) measured were above 0.6 and below 14%, respectively, indicating that the assays established on the 384-pillar plate are robust and reproducible.

TABLE OF CONTENTS

LIST OF TABLES

LIST OF FIGURES

CHAPTER I

INTRODUCTION

High attrition rates of drug candidates in clinical trials and increases in societal concerns for animal welfare have driven *in vitro* and in silico human toxicology testing innovations [1]. Lead compounds selected for traditional high-throughput screenings (HTS) using two-dimensional (2D) cell monolayers and preclinical evaluations with animal models are often inaccurate due to lacking correlations between *in vitro* cell-based models and *in vivo* models and differences in genetic makeup between animals and humans. The poor predictivity of *in vitro* models to *in vivo* models is due to a lack of drug metabolism in these systems. Drugs are primarily metabolized in the liver by a variety of drug-metabolizing enzymes (DMEs), including cytochromes P450 (CYP450s), UDP-glucuronosyltransferases (UGTs), sulfotransferases (SULT), glutathione S-transferases (GSTs), etc. [2][3]. These DMEs are involved in the initial clearance of drugs from the body and generate drug metabolites; however, some of these compounds are unstable and toxic, leading to undesirable biological consequences, not only in the liver, but in other organs as well [4][5]. Inter-individual variability in DMEs levels and polymorphisms result in significant diversity for drug metabolism, which eventually leads to differences in the

response of patients to drugs and their adverse drug reactions (ADRs) [6][7]. Therefore, maintaining physiologically relevant levels of DMEs in HTS assays and understanding the roles of these enzymes in drug metabolism are essential in human toxicology testing. However, incorporating physiological levels of chemical metabolism into traditional HTS assays are still challenging, as addressed in "The Transform Tox Testing Challenge: Innovating for Metabolism" (TTTC) promoted by the EPA and the National Institutes of Health (NIH) subsidiaries, such as the National Center for Advancing Translational Sciences (NCATS) and the National Institute for Environmental Health Science (NIEHS).

To address drug metabolism issues and develop better predictive toxicity assessment tools, the National Toxicology Program (NTP), housed within the NIEHS, has led the innovation in high-throughput *in vitro* assays. The data generated from the ToxCast and Tox21 programs demonstrated methods to evaluate and prioritize the toxicity of chemicals using a panel of assays and provided potential insight into chemical toxicity *in vivo* [8][9]. In addition, the European Union Reference Laboratory for Alternatives to Animal Testing (EURL ECVAM) of the European Commission's Joint Research Centre has published an article on the possible use of a simple modelling approach to avoid the use of chronic fish testing in chemical risk assessment [10]. The EU policies on endocrine disruptors, multiple efficacy of chemicals, and nanomaterials are good examples, demonstrating that traditional risk assessment is coming to an end. The EURL ECVAM intensely participates in the research of the replacement, reduction or refinement (3R) of laboratory animals using alternative tests [11]. Alternative test methods developed by research laboratories have been submitted to the EURL ECVAM for reliability, robustness, and predictivity to be widely accepted as new tools for hazard and risk assessment [10].

In response to this need, we have been making important contributions to metabolism-induced toxicity assessment by using several microarray chip platforms, including the metabolizing enzyme toxicology assay chip (MetaChip), the data analysis toxicology assay chip (DataChip), and the transfected enzyme and metabolism chip (TeamChip) [12-14]. However, these microarray chip platforms were too small in size for robotic systems commonly adopted for HTS assays and require difficult retrofitting for existing HTS assays. Thus, we have developed a new 384-pillar plate that can be coupled with standard 384-well plates for 3D cell cultures and high-throughput, high-content imaging (HCI) assays (Figure 1). This 384-pillar plate can be sandwiched with standard 384-well plates, compatible with existing HTS equipment such as microtiter plate readers, which allows for rapid absorbance, fluorescence, and luminescence measurements *in situ* (Figure 2). By demonstrating cell printing technology on the 384-pillar plate, we participated in Stages I and II of the Transform Tox Testing Challenge. To rapidly predict metabolism-induced toxicity of compounds, we printed human embryonic kidney (HEK) 293 cells in a mixture of alginate and Matrigel on the 384-pillar plates using a microarray spotter, which were coupled with a 384-well plate containing model compounds from the EPA and DMEs. Representative DMEs, including CYP3A4, CYP1A2, CYP2B6, CYP2C9, CYP2D6, CYP2E1, and UGT1A4, have been used to emulate metabolic reactions in the human liver and evaluate augmented toxicity and detoxification by metabolism of the compounds.
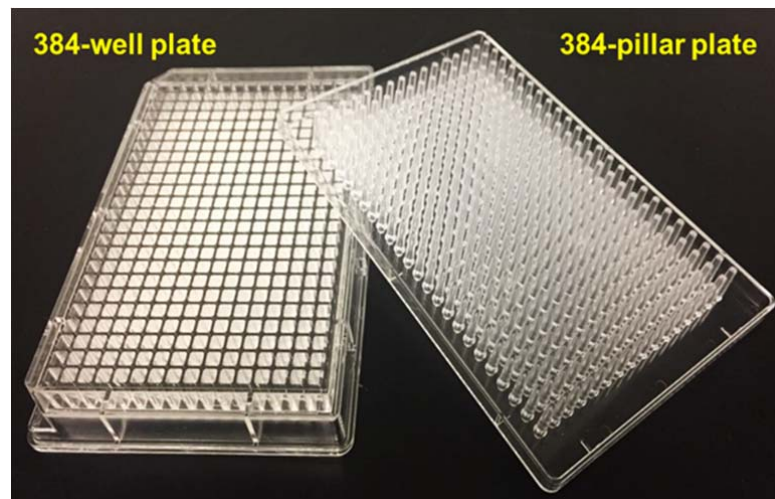
Figure 1. Picture of the 384-pillar plate and the 384-well plate.

Sandwiching for incubation
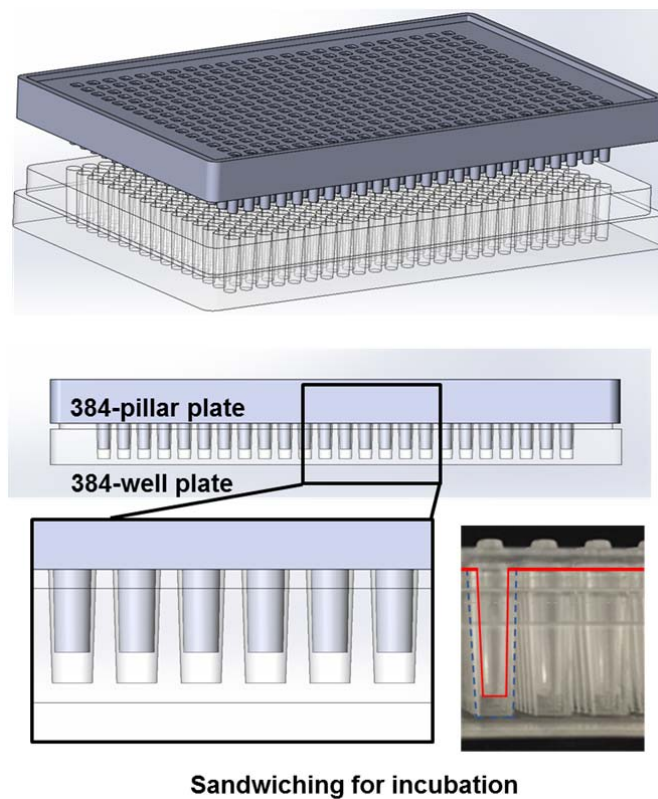
Figure 2. The sandwiched 384-pillar/well plate. The close-up image shows the cut plane of the sandwiched plate.

CHAPTER II

LITERATURE REVIEW

2.1 Chemical Toxicity Testing

In the past year, more than 85,000 chemicals have emerged in the United States [Toxic Substance Control Act Inventory List]. Although the number of new chemicals continues to increase, most of these have yet to be adequately tested for their effects on human health. Chemical toxicity is generally evaluated by using animal-based test methods, which have provided useful information on the safety of chemicals [15][16]. However, these traditional methods are relatively expensive and low throughput, which make it difficult to define the mechanism of action, and continue to face mounting ethical concerns [17]. Furthermore, intra- and inter-species differences make it difficult to extrapolate results to human outcomes [18]. Thus, there is great interest in alternative test models for measuring potential toxicities of new chemicals. The National Research Council (NRC) recognized the dramatic advances in molecular and cellular biology and proposed a new roadmap in 2004, 'A National Toxicology Program for the 21st Century.' This roadmap focuses on three main areas: refining traditional toxicology

assays, developing rapid mechanism-based predictive systems, and improving the overall quality of data for making public health decisions. This plan placed an increased emphasis on *in vitro* systems for identifying key mechanisms of chemicals [19]. The U.S Environmental Protection Agency (EPA) faced the same difficulty of evaluating chemical toxicity and launched the ToxCast program in 2007 [20]. ToxCast is currently in its third and final phase, during which it has tested over 1800 possibly hazard compounds [20][21]. The goal of the program is to evaluate the toxicity of thousands of chemicals using automated HTS technologies. HTS has been developed by the pharmaceutical industry to evaluate the biological mechanisms of drug candidates [22]. HTS technology optimized for drug discovery is now being transferred to toxicological screening, representing a new paradigm in toxicological testing [23]. However, ToxCast assays have two major pitfalls. First, ToxCast assays are extremely limited in their ability to determine the effects of metabolism on chemical toxicity. In other words, ToxCast assays are not able to measure how a chemical might change in toxicity (i.e., become more or less toxic) as it is processed by our bodies. Second, ToxCast assays are limited in their ability to analyze the full range of chemical compounds. For example, chemicals that are not soluble in the solvent dimethyl sulfoxide (DMSO), such as heavy metals, make high-throughput analysis more difficult.

To resolve these issues and continue working on the ToxCast results, the Toxicology in the 21st century (Tox21) program was developed with several federal agencies: the US EPA, the NIH, the NIH Chemical Genomics Center (NCGC), the NTP, and the Food and Drug Administration (FDA). With this combined expertise, over 12,000 compounds were screened [24]. Both programs have generated a broad spectrum of high-throughput/high-content biochemical and cell-based data used to

predict *in vivo* toxicity endpoints [25]. The ToxCast and Tox21 purposes were to create *in vitro* "signatures" that are relevant to *in vivo* toxicity and to develop biologically predictive models based on multiple HTS assays. Combining computational toxicology and *in vitro* models provide a complement approach to identify untested environmental chemical toxicities as an alternative to animal models for chemical safety evaluation [26]. The purpose of these programs was to move toxicology from a predominantly observational science at the disease specific level to a predominantly predictive science focused on a broad inclusion of target-specific, mechanism-based biological observations. The EPA established the TTTC with the goal of incorporating physiological levels of chemical metabolism into conventional HTS assays to better predict toxicity of parent compounds and their metabolites *in vivo*.

2.2 The Role of the Liver in Drug Metabolism

When chemicals are ingested or inhaled by living organisms, the liver is the "first pass" organ for administered compounds [27]. The liver, which is mainly composed of hepatocytes, contains a wide variety of enzymes to process a myriad of chemicals [28]. The term metabolism used here is to define all transformations of drugs and chemicals by an enzyme(s) [29]. Metabolism of environmental chemicals is composed of two different phases. Phase I reactions involve the modification of compounds, where hydrolysis is the most common [28]. Phase II reactions involve conjugation reactions by transferases, which play a crucial role in increasing the solubility of compounds in order to facilitate excretion out of body [30-32]. Metabolism of chemicals is highly affected by drug-metabolizing enzymes (DMEs) and their isoforms. Thus, knowledge in the role of DMEs in metabolism is an important area to assess human toxicology testing.

2.2.1 Phase I

Cytochrome P450 (CYP450s) enzymes are a family of monooxygenases and play a crucial role in phase I metabolism by performing oxidation, reduction, and hydrolysis [28][29]. CYP450 enzymes mostly focus on the initial modification of drugs, which decrease the plasma concentration and affect the bioavailability [28][29]. During this process, phase I metabolites are generated, some of which are biological activity to perform desired pharmacological effects [33][34]. On the other hand, interactions of DMEs with drugs or other chemicals can inhibit other enzymes, leading to severe toxicity or even death [35]. Furthermore, levels of CYP450 enzymes vary among individuals, leading to broad variations of drug efficacy [36]. DMEs typically exist in a variety of isoforms. Isoforms are enzymes that share the same general reaction mechanism, but are encoded for by different genes [37]. Within as many as 18 families of DMEs, there are important subfamilies and isoforms that have substantial involvement in metabolism during drug exposure. Of the P450s, CYP1A2, CYP2C9, CYP2C19, CYP2D6, and CYP3A4 account for the majority of drug metabolism, with additional contribution from CYP2E1, CYP2A6, CYP2C8, and CYP2B6 [38-40]. However, CYP450 enzymes involved in chemical metabolism can be dangerous. Oxidation by CYP450 enzymes can also convert a parent compound into a more highly toxic metabolite, such as a carcinogen [29][33]. Biologically reactive intermediates by CYP450 enzymes, such as epoxides, hydroxylamines, acyl halides, can attach to deoxyribonucleic acids (DNA) or proteins, causing cell damage because of their inherent instability [41]. Compared to drug metabolism, CYP1A1, CYP1A2, CYP1B1, CYP2A6, CYP2E1, and CYP3A4 were reported to have a greater contribution to carcinogen activation rather than drug metabolism [42]. Thus,

understanding of CYP450 enzymes is important in drug metabolism and chemical toxicology.

2.2.2 Phase II

In Phase II, subsequent conjugation reactions (e.g. glucuronidation, sulfation, acetylation, and the addition of amino acids and peptides, including glutathione, are carried out by phase II enzymes, such as UDP-glucuronyltransferases (UGTs), glutathione S-transferases (GSTs), sulfotransferases (SULTs), methyltransferases, and aryl-amine N-acetyltransferases (NATs). Phase II biotransformation mostly leads to detoxification of reactive metabolites and results in increased hydrophilicity, allowing excretion of these metabolites via transporter proteins of hepatocytes [30][43]. For example, GST catalyzes the conjugation of reduced glutathione to various bioactivated metabolites generated by CYP450 enzymes, resulting in detoxification of the active metabolites [43]. In another example, UGT catalyzes the conjugation of D-glucuronic acid to metabolites possessing carboxylic acid groups [43]. Both of these reactions account for the majority of detoxification of reactive metabolites.

2.3 Existing *In Vitro* Toxicity Test Platforms

Currently, animal models are widely used for the prediction of *in vivo* drug metabolism. However, animal models cannot correctly reflect the *in vivo* conditions due to interspecies differences. In addition, animal models are difficult to use in HTS, due to cost. Therefore, there is need for a novel, efficient, inexpensive model, which can be applied for drug toxicity screening. In this decade, *in vitro* modeling has been largely improved. *In vitro* models are cost-effective and suitable for large-scale screening.

2.3.1 Traditional Liver-Derived *In Vitro* Systems

Over the past few decades, liver-derived *in vitro* model systems have been developed to provide insights into *in vivo* drug metabolism and toxicity. Liver tissue slices, primary hepatocytes, and immortalized cell lines are extensively used for *in vitro* models of liver toxicity testing. Advantages and disadvantages of these systems vary greatly.

Liver tissue slices can retain liver structure and preserve all the cell types found *in vivo*. Thus, it is an appropriate system to correlate metabolism *in vitro* to *in vivo* [44]. Liver slice models are stable for 20-96 hours, with slightly decreased phase II enzyme activity and albumin production [45][46]. However, metabolic enzyme levels are greatly reduced after 6-72 hours and cellular necrosis occurs after 48-72 hours [47-49]

Primary hepatocytes cultures are considered to be the gold standard for *in vitro* toxicity testing [50]. Primary hepatocyte cultures can retain morphology and complete liver-specific functionality, such as DMEs, similar to *in vivo* situations for the short term [51]. Therefore, primary hepatocyte cultures have been used for *in vitro* studies such as enzyme induction, inhibition, and drug testing [52]. Nevertheless, primary hepatocytes cultures are expensive and difficult to obtain in large quantities with uniform cell function for large scale toxicity screening. In addition, these models have drastic morphological alterations and rapid loss of liver-specific functions with variable expression levels of DMEs when the cells are maintained in monolayer cultures [51][53]. After the cell loses liver specific functions, response to chemicals are different to *in vivo*.

To maintain liver-specific functionality over long periods of time, a simple sandwich culture was introduced. In this system, hepatocytes are placed between two

layers of matrix (traditionally collagen or Matrigel®) [54]. This configuration prevented the loss of cell viability, increased enzyme activities, and mimicked *in vivo* conditions [54][55]. With this platform, liver-specific functionalities or positive effects are maintained for extended periods of time due to contributions of the extracellular matrix (ECM) [54].

Commercially available immortalized liver-derived cell lines include HepG2, Hep3B, and HepaRG [56][57]. The advanced cell line, HepaRG, derived from a human hepatocellular carcinoma, can differentiate into both the biliary and hepatocyte lineage. HepaRG cells have expression levels of liver-specific functions, including CYPs and phase II enzymes [58]. HepaRG retains a high proliferative capacity and improved reproducibility for experiments [58][59]. HepaRG represents a phenotype derived from a single donor, thereby reducing its predictive value for inter-individual variances [58].

2.3.2 Novel *In Vitro* Toxicity Test Platforms

With progress in the manufacturing of micro-scale channels on biocompatible plastics, such as polydimethylsiloxane, microfluidic platforms have become valuable for *in vitro* toxicity testing [60][61]. The semi-automated system called the HepaChip®, is a highly advanced microfluidic system mimicking hepatic sinusoids with two electrodes [62]. Schutte et al. were able to demonstrate that hepatocytes from HepaChip® had a higher activity of DMEs, compared to those co-cultivated in 96-well plates [62]. While small volumes are required, it is limited due to its complex system of tubing lines and reservoirs. A major advantage of microfluidic devices over other platforms is its ability to emulate physiological conditions *in vitro* by providing mechanical stress, nutrient exchange, and drug exposure [61]. The microfluidic device was able to maintain 3D tissue-like cellular morphology and cell-specific

11

functionality of human hepatocytes [63]. However, these sophisticated systems will have difficulty when being adjusted for high throughput [61].

Several bioreactors have been developed for toxicology studies with hepatocytes [64]. Schmelzer et al. utilized a hollow-fiber bioreactor where cells are seeded into the extracapillary space and are surrounded by three independent capillary membrane systems [65]. The capillary systems are composed of porous polyethersulphone and hydrophobic multilaminate hollow fiber membranes, which allow for gas exchange. The capillary layers are interwoven around the extracapillary space and two of the capillary systems are perfused in a counter-current flow with culture medium or plasma, while the third allows for decentralized oxygenation and supply of nutrients. Oxygen delivery to hepatocytes is essential to retain of liver-specific functions. When the cells are exposed to low oxygen concentrations, gene expression related to liver-specific functions rapidly was decreased [66]. Hollow fiber bioreactors increased expression of phase I and phase II enzymes and transporters [67-70]. Miranda et al., were able to demonstrate that hepatocytes cultured in small stirred bioreactors allow for improved functionality [71]. The bioreactors also allow for a well-defined culture environment with control culture parameters, such as pH and temperature [72][73]. The main disadvantage of bioreactors is that they required a high number of cells and large amounts of reagents, increasing costs. More recent developments concentrate on the miniaturization for routine application in research.

2.4 Mechanisms of Toxicity of Model Compounds

In the following section, we will discuss the mechanisms of toxicity of the model compounds used in our experiment. The nine model test compounds, benzo[a]pyrene, aflatoxin B1, cyclophosphamide, 2-naphthlyamine, acrylamide, doxorubicin hydrochloride (HCl), 6-aminochrysene, 8-methoxypsoralen, and 4-

nitrophenol were provided by the EPA. Prior to testing model compounds, acetaminophen was used to measure the error range and the quality of the new assay. The model compounds were selected from a wide range of carcinogens to chemotherapy agents to induce various mechanisms of toxicity so that we could demonstrate our ability to detect metabolism-induced toxicity on the 384-pillar plate.

2.4.1 Acetaminophen

Acetaminophen (APAP) is widely known to be an analgesic and antipyretic medication. When APAP is ingested, there are two phases of APAP metabolism. The majority of APAP is metabolized via CYP450s, particularly CYP2E1, CYP1A2, and CYP3A4, to N-acetyl-p-benzoquinone imine (NAPQI), which is a highly reactive toxic metabolite [74][75]. NAPQI can bind to membrane proteins, resulting in oxidative stress and mitochondrial dysfunction. This leads to the disruption of adenosine triphosphate (ATP) production, ultimately causing cell necrosis [76][77]. Another portion of APAP is neutralized via the phase II enzymes UGT and SULT to form glucouronidated and sulfated conjugates that can be eliminated from the body through urine [78].

2.4.2 Benzo[a]pyrene

Benzo[a]pyrene (BAP) is a carcinogen categorized as a poly-cyclic aromatic hydrocarbon (PAH) [79]. PAH are initially lipophilic and inert, but can be activated to become reactive molecules by DMEs [80]. The metabolism of BAP is defined by its several conversions through CYPs subfamilies and epoxide hydrolase [79][80]. BAP is first oxidized to Benzo[a]pyrene-7,8-oxide by CYP1A2, CYP2C9, and CYP3A4 [79-82]. Then benzo[a]pyrene-7,8-diol is produced by opening the epoxide ring [83]. Benzo[a]pyrene-7,8dihydrodiol-9,10-epoxide is the ultimate product of BAP through

enzymatic reactions [80]. This final molecule binds to DNA and can introduce mutations, ultimately becoming a carcinogenic process [79].

2.4.3 Aflatoxin B1

Aflatoxins are mycotoxins produced by fungi in the genus Aspergillus, like *Aspergillus flavus* [84]. There are over 20 isolated aflatoxin derivatives produced by several fungal species [84]. Aflatoxins cause acute and chronic effects after human or animal consumption [85, IARC (1993)]. Aflatoxin B1 (AFB1) is the most toxic with respect to the cytotoxic effects among the known mycotoxins [84][85]. AFB1 has been demonstrated to cause oxidative damage in cultured rat hepatocytes, leading to cell injury [86]. In the human liver, CYP3A4 and CYP1A2 play important roles in the biotransformation of AFB1 [87]. CYP3A4 is an important enzyme that catalyzes the reaction of AFB1 to AFB1-8,9-epoxide (AFBO), while CYP1A2 catalyzes the reaction of AFB1 to Aflatoxin Q1 (AFQ1) [88]. The epoxide can be conjugated with glutathione [88][89]. AFM1 and AFM2 are the metabolites formed by the hydroxylation of AFB1 [90]. AFM1 is considered a detoxified product [91]. Another study demonstrated AFB1 was found to be more toxic than AFM1 on intestinal cells both before and after differentiation in Caco-2 cells, leading to membrane damage [92].

2.4.4 Cyclophosphamide

Cyclophosphamide (CPA) is commonly used as an anticancer agent against breast cancer and lymphomas [93]. CPA itself is a prodrug, meaning it is therapeutically inactive. Thus, metabolites of CPA have been investigated [93]. Cyclophosphamide is initially hydroxylated to 4-hydroxycyclophosphamide and aldophosphamide, eventually leading to the generation of the therapeutically active phosphoramide mustard and the toxic by-product, acrolein [93][94]. Oxidation of

CPA occurs through one or more of the CYPs isoforms [95][96]. CYP2B6 displayed the highest activity in CPA 4-hydroxylation activity, followed by CYP3A4 and CYP2C19. CYP1A1, CYP2C9, and CYP3A7 contributed to low rates of CPA 4-hydroxylation [96][97]. CYP3A4 is also involved in N-dechloroethylation, another oxidative pathway [97].

2.4.5. 2-Naphthylamine

2-Naphthylamine (2-NA) is classified as a bladder carcinogen found in cigarette smoke [98][99]. 2-NA is metabolized via N-hydroxylation and N-glucuronidation in the liver and its N-glucuronide is transported to the urinary bladder [100]. 2-NA is metabolized via N-hydroxylation by CYP1A2 to N-hydroxy-2-naphthylamine (N-OH-NA). N-OH-NA and 2-Amino-1-naphthol generate reactive oxygen species and causes damage to DNA [101]. Enzymes in the UDP-glucuronosyltransferase 1 family, including UGT1A4, can convert 2-NA and 2-Hydroxyamino-naphthalene to form 2-Naphthylamine-N-beta-D-glucuronoside and 2-Hydroxyamino-naphthalene-N-beta-D-glucuronoside,respectively [100-103].

2.4.6 Acrylamide

Acrylamide (AA) has been detected in high concentrations in fried and baked starch-enriched food [104]. AA is known to be a potential carcinogen in humans and rats [105][106]. Glycidamide (GA) is a metabolite of acrylaminde and has been demonstrated to cause somatic cell mutagenicity in *in vivo* studies [107]. CYP2E1 in the human liver is a major player in the production of GA [108]. Kurebayashi et al. has shown that GA is more toxic than AA by measuring the decrease in hepatocyte viability [109]. Koyama et al. has also identified that GA is much more reactive with DNA than AA [110]. GA can be further conjugation, resulting in the formation of N-acetyl-S-

(carbamoyl-2-hydroxyethyl)cysteine and N-(R,S)-acetyl-S-(2-hydroxy-2-carbamoylethyl)-cysteine by several GSTs [111-112].

2.4.7 Doxorubicin HCL

Doxorubicin (DOX), an anthracycline glycosidic anticancer drug, impairs DNA synthesis during tumor cell division and is used for the treatment of lymphoma, osteosarcoma, and other cancers [113]. DOX is metabolized to doxorubicinol and both can be metabolized to their aglycones, doxorubicinone and 7-deoxydoxorubicinone, respectively, by cytoplasmic NADPH-dependent aldo-keto reductase [114-116]. Doxorubicinol is a more cardiotoxic metabolite of DOX [117].

2.4.8 6-Aminochrysene

6-Aminochrysene (6-AC) is characterized as a potent mutagen and metabolized by liver CYP450S to N-hydroxylated metabolites and epoxide intermediates [118][119]. 6-AC is bioactivated through two pathways (N-hydroxylation and epoxidation). 6-AC is mainly transformed by CYP450s via N-hydroxylation pathways. These conjugation reactions are followed by N-acetyltransferases, forming carcinogenic products [120]. Another reaction is the diolepoxide pathway. By using S. typhimurium TA1535/pSK1002, Shimada et al. have proven that CYP3A4 is the most important isoform involved in 6-AC activation [121]. Yamazaki et al. have shown that CYP2B6 and CYP3A4 are involved in actively transforming 6-AC to form reactive N-hydroxylated products, whereas CYP1A2 catalyzes 6-AC through the diolepoxide pathway [122][123]

2.4.9 8-Methoxypsoralen

8-Methoxypsoralen (8-MOP) has been used as a photochemotherapeutic agent, treating various skin diseases, including psoriasis [124]. 8-MOP metabolism in human is characterized by the formation of 8-hydroxypsoralen. Deeni et al. revealed

that CYP1B1 is abundant in human skin and is the key contributor to 8-MOP metabolism [125]. They showed CYP1A1, CYP1A2, CYP1B1, CYP2A6 and CYP2E1 influence 8-MOP metabolism by using E.coli membranes co-expressing various CYP450s and CYP450 reductase.

2.4.10 4-Nitrophenol

4-Nitrophenol (4-NP) is commonly used as pesticide [126]. Ingested or inhaled 4-NP is hydroxylated to form 4-nitrocatechol (4-NC) by CYP2E1 [127]. A major role of the CYP2E1 in 4-NP hydroxylation in laboratory animals has been demonstrated [128][129]. CYP2E1 is involved in the hydroxylation of 4-NP to 4-NC in at least 85% of humans [127]. Zerilli et al. used individual CYP450s (CYP2E1, CYP3A4, CYP3A5, and CYP2A6) with human β-lymphoblastoid cells to demonstrate hydroxylation of 4-NP in the presence of cytochrome b5, a stimulator. CYP2E1 was found to be the most sensitive isoforms [130]. The ability of CYP3A4 was shown to metabolize 4-NP somewhat when complexed with cytochrome b5 [130].

2.5 Endpoints

Various mechanisms (such as redox potential, integrity of cell membrane, and activity of cellular enzymes) were assessed to detect cell viability. Each factor indicates a different aspect of cell health, which can be used to assess and quantify cell viability. Indicators for cell viability have been developed to make them compatible with fluorescence microscopes, microplate readers, or flow cytometers, and have sensitivity, specificity, and compatibility for different cell lines.

2.5.1 Cell Membrane Integrity

Calcein acetomethoxy diacetylester (Calcein AM) is a well-known fluorescent cell permeant dye used to measure cell viability or cytotoxicity [131]. Calcein AM has enhanced hydrophobicity compared to Calcein, allowing passive

diffusion through viable cell membranes. After Calcein AM permeates into the cytoplasm, it is hydrolyzed by intracellular esterases to Calcein, which is a green fluorescent compound. Fluorescent cells indicate intact cell membranes. Calcein does not inhibit any cellular functions, such as proliferation. Calcein is detected with the excitation/emission spectra of 495/515 nm.

2.5.2 Cellular ATP Levels

Mitochondria are found in all eukaryotic cells and are responsible for generating ATP, playing a central role in living processes as an energy source. Measuring ATP levels is a fundamental method to detect viability [132]. Historically, firefly luciferases extracted from Photinus pyralis (LucPpy) have been used for ATP assays [133][134]; however, LucPpy luciferase has only moderate stability *in vitro* and is sensitive to environmental factors, such as pH. These characteristics prevent its potential of developing a robust homogenous ATP assay. However, Promega has successfully established a stable form of luciferase purified from Photuris pennsylvanica (LucPpe2). Luciferases from LucPpe2 show improved stability, improving the robustness of the assay. During cell death, levels of ATP drop rapidly as metabolism shuts down and ATP is degraded by endogenous ATPases. The CellTiter-Glo$^®$ assay generates a stable luminescent signal while simultaneously blocking the activity of ATPases during cell lysis. The assay uses the luciferase reaction to measure ATP as an indicator of metabolically active cells [133][134]. The enzyme luciferase acts on luciferin in the presence of Mg^{2+} and ATP to provide oxyluciferin, which emits energy in the form of luminescence [133]. Generation of a luminescent signal is proportional to the amount of ATP present, indicating cellular metabolic activity. The CellTiter-Glo$^®$ assay allows us to quickly and efficiently

detect luminescence for HTS. Detection of cell viability with luciferase and biochemical markers are powerful tools for identification of compound mechanisms.

2.6 Dose-Response Curves

The effects of DMEs can be plotted using a graph representing the concentration of the compound versus the physiological effect, also known as a dose response curve. To understand the effect of compound metabolites on the cells, the logarithm of test compound concentration is plotted on the x-axis, while the physiological response from different mechanisms is plotted on the y-axis. Dose-response curves are able to show the IC_{50} values, which represent the concentrations of compounds where 50% of the biological cellular response is inhibited.

CHAPTER III

METHODS

3.1 Culture of Human Embryonic Kidney (HEK) 293 Cells in T-75 Flasks

As a target cell model to evaluate the performance of metabolism-induced toxicity, HEK 293 cells from the American Tissues Culture Collection (ATCC, Rockville, MD, USA) were used in Stage II of the TTTC. HEK 293 cells were cultured in Dulbecco's modified eagle medium (DMEM, Corning, Corning, NY, USA) supplemented with 10% fetal bovine serum (Corning) and 1% penicillin/streptomycin (Gibco, Gaithersburg, MD, USA) in T-75 flasks in a 5% CO_2 incubator at 37°C and passaged when it is around 80% confluent. Cell suspensions were prepared by adding 2 mL of 0.25% trypsin in the T-75 flask, incubating for 2 - 3 minutes at 37°C, adding 7 mL of growth media, breaking apart big cell clumps by rigorous aspiration and dispensation, centrifuging at 500 x g for 3 minutes to form a cell pellet, removing the supernatant gently, and re-suspending the cells with 2 mL of growth media. The cell number was counted with a Moxi Z automated cell counter by loading 75 µL of the cell suspension in a Moxi Z cassette.

3.2 Culture of HEK 293 Cells in 3D on 384-pillar Plates

To ensure robust cell spot attachment to the 384-pillar plate (Medical & Bio Device (MBD), Republic of Korea), the surface of the 384-pillar plates was coated with 0.01% (w/v) poly (maleic anhydride-*alt*-1-octadecene) (PMA-OD from Sigma-

20

Aldrich, St. Louis, MO, USA). Briefly, a 0.01% (w/v) PMA-OD working solution was prepared in 50 mL conical tubes by diluting 0.1% (w/v) PMA-OD dissolved in ethanol 10-fold with ethanol and proper mixing. The 384-pillar plates were immersed in 20 mL of the 0.01% (w/v) PMA-OD in the lid of a 384-well plate and then dried in a sterile bioassay plate at room temperature for 2 - 3 hours. For robust spot attachment by ionic interactions and gelation with alginate, a 2 µL mixture of 0.0033% poly-L-lysine (PLL from Sigma-Aldrich) and 16.66 mM barium chloride ($BaCl_2$ from Sigma-Aldrich) was printed on each pillar of the PMA-OD-coated 384-pillar plate using a microarray spotter (S+ MicroArrayer from Advanced Technology Inc. (ATI), Incheon, South Korea). After drying overnight, 1.5 µL of the HEK 293 cell suspension in a mixture of 0.75% low-viscosity alginate (Sigma-Aldrich) and 1 mg/mL growth factor reduced (GFR) Matrigel (Corning) at 0.67×10^6 HEK 293 cells/mL was printed on each pillar of the PLL-$BaCl_2$-treated 384-pillar plate using the S+ MicroArrayer (Figure 3). After 4 minutes of gelation on the chilling deck of the S+ MicroArrayer, the 384-pillar plate containing 1000 HEK 293 cells per pillar was sandwiched with a 384-well plate containing 60 µL of complete DMEM growth medium supplemented with 10% FBS and 1% P/S in each well. After pre-incubation for 4-6 hours to remove excess $BaCl_2$, the 384-well plate containing the complete growth medium was discarded and the 384-pillar plate was sandwiched overnight with a new 384-well plate containing 40 µL of the complete DMEM growth medium supplemented with 50 µM buthionine sulfoximine (BSO) in each well. BSO, which is an inhibitor of gamma-glutamylcysteine synthetase, was supplemented in the growth medium to reduce cellular levels of glutathione and increase the sensitivity of reactive metabolites generated by DMEs [14].
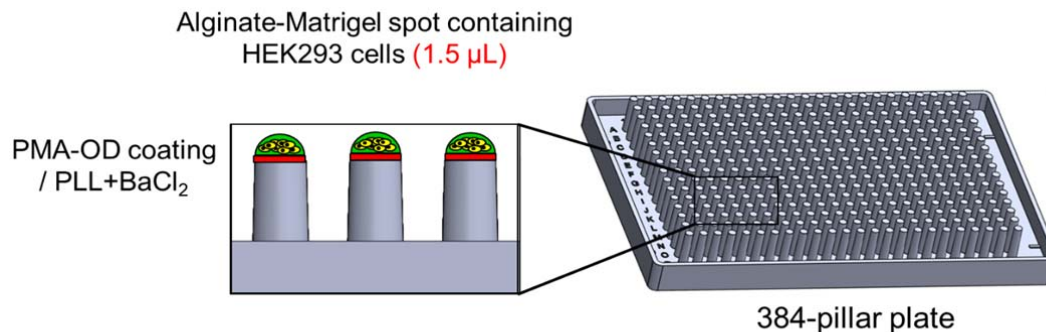
Figure 3. Schematic of the 384-pillar plate for 3D cell culture.

3.3 Measurement of DME Activity

Prior to metabolism-induced toxicity assays with HEK 293 cells, we confirmed activities of the DMEs with fluorogenic substrates. For CYP450 activity assays, 2 mM stock solutions of fluorogenic substrates, including BOMCC (for CYP2B6, CYP2C9, and CYP3A4, Invitrogen, Carsbad, CA, USA) and EOMCC (for CYP1A2, CYP2D6, and CYP2E1, ThermoFisher) were prepared in acetonitrile. A CYP450-NADP-regeneration system mixture of 1000 nM CYP450 isoform (ThermoFisher), 10 mM NADP$^+$ (ThermoFisher) in 100 mM potassium phosphate buffer (pH 8.0), and Vivid$^®$ regeneration system (100X from ThermoFisher) containing 333 mM glucose-6-phosphate and 30 U/mL glucose-6-phosphate dehydrogenase in 100 mM potassium phosphate buffer (pH 8.0) was prepared at a ratio of 2:1:1. The fluorogenic substrates were diluted 200-fold in complete DMEM to prepare a final 10 μM of the substrates. For enzymatic reactions, 47.5 μL of 10 μM BOMCC (or 10 μM EOMCC) was added into 384-well plates, which was followed by adding 2.5 μL of the CYP450-NADP-regeneration system mixture (final enzyme concentrations can be found in Table 1). The fluorescence intensity was immediately recorded using a microtiter plate reader (Synergy H1, BioTek instruments, Winooski,

22

VT, USA) at an excitation wavelength of 405 nm and an emission wavelength of 460 nm.

For the UGT activity assay, a 100 μM 4-methylumbelliferone (4-MU, Sigma-Aldrich) working solution was prepared by mixing 1 μL of the stock 100 mM 4-MU in methanol with 1 mL of complete DMEM. For the enzymatic reaction, 30 μL of the 100 μM 4-MU was mixed with 1 μL of UDPGA (Corning) into 384-well plates, which was followed by adding 2.5 μL of 5 mg/mL UGT1A4 (Corning). The fluorescence intensity was immediately recorded using the microtiter plate reader at an excitation wavelength of 372 nm and an emission wavelength of 445 nm.

Table 1. Activity of representative drug metabolizing enzymes (DMEs) and their substrates.

Enzymes	Substrates	Substrate conc. (μM)	Enzyme conc. [E0]	Initial rate measured (RFU/min)	Initial rate/[E0]	Literature K_m (μM) [a]	Literature V_{max} (nM/min) [a]
CYP1A2	EOMCC	10	38 nM	655	26	3	5
CYP2B6	BOMCC	10	38 nM	640	26	51	87
CYP2C9	BOMCC	10	38 nM	21	1	13	1
CYP2D6	EOMCC	10	38 nM	52	2	43	5
CYP2E1	EOMCC	10	75 nM	45	1	20	5
CYP3A4	BOMCC	10	38 nM	277	11	10	95
UGT1A4	4-MU	100	0.38 mg/mL	3045	8013	61	1500 [b]

[a] The K_m and V_{max} values were obtained from the Vivid CYP450 screening kit protocol provided by Thermo Fisher Scientific.
[b] pmol/min/mg

3.4 Preparation of 384-well Plates Containing Test Compounds and Drug Metabolizing Enzymes

HEK 293 cells on the 384-pillar plate were exposed to different concentrations of compounds and DMEs. The nine test compounds, benzo[*a*]pyrene, aflatoxin B1, cyclophosphamide, 2-naphthlyamine, acrylamide, doxorubicin hydrochloride (HCl),

6-aminochrysene, 8-methoxypsoralen, and 4-nitrophenol, were obtained from the EPA. The highest dosage of the compounds tested was 250 µM, by creating a 1:200 dilution of the 50 mM compound stock solutions in DMSO with 50 µM BSO-supplemented DMEM. Using the highest dose, 2-fold serial dilutions of the compound were performed with 50 µM BSO-supplemented DMEM containing 0.5% DMSO in 1.5 mL Eppendorf tubes. Eight dosages at 1:200, 1:400, 1:800, 1:1600, 1:3200, 1:6400, 1:12800, and 1:25600 dilution and one solvent-alone control (DMSO control) were prepared for each compound. A single compound was serially diluted and then added in sections 1 – 9 of the 384-well plate, with section 1 being a DMSO only control (Figure 4).
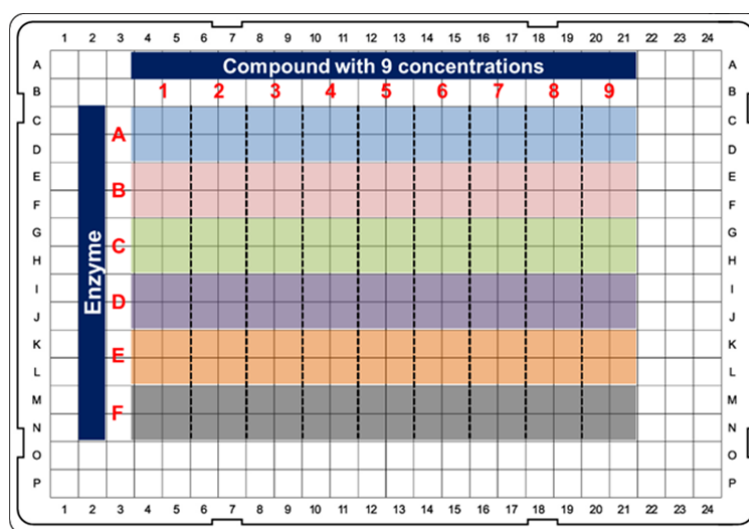
Figure 4. Layout of the 384-well plate (216 spots/plate) for *in-situ* drug metabolism.

For Phase I DME reactions, CYP450 solutions, including CYP3A4, CYP1A2, CYP2B6, CYP2D6, CYP2E1, CYP2C9 (ThermoFisher), were prepared in 96-well plates by mixing 125 µL of 1000 nM CYP450, 62.5 µL of 10 mM $NADP^+$, and 62.5 µL of Vivid® regeneration system (100X) on ice until use. Baculosome® Plus was used as a no enzyme control (ThermoFisher). For Phase II DME reactions, the UGT

Reaction Mix A (25 mM UDPGA from Corning) was diluted with 50 µM BSO-supplemented DMEM to prepare a final 0.75 mM UDPGA solution. This was followed by preparing a mixture of UGT1A4 solution using 2.5 µL of 5 mg/mL UGT1A4 (Corning) and 31 µL of 0.75 mM UDPGA.

Finally, 30 µL of each dilution of compound were dispensed in a 384-well plate using a multichannel pipette and 2.5 µL of the five DMEs and one baculosome[®] control were printed in 6 regions of the 384-well plate (Figure 4). As shown in Figure 4, region A specifically contained the baculosome[®] control as a test compound only control; regions B - E contained 4 CYP450 isoforms; and region F contained UGT1A4 as a representative phase II enzyme. The 384-pillar plate with HEK 293 cells was then sandwiched with the 384-well plate containing one test compound and DMEs and incubated in the 5% CO_2 incubator at 37°C for 24 hours (Figure 5). This was repeated for all test compounds.
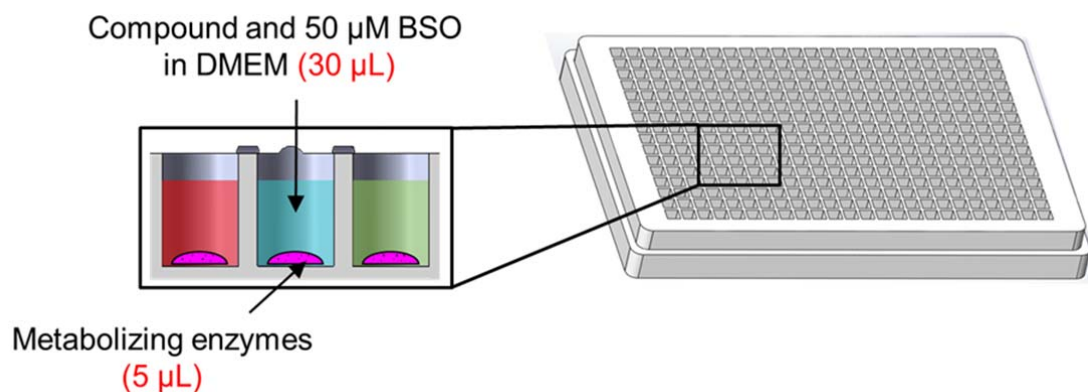
Figure 5. Schematic of the 384-well plate containing single compound with DMEs.

3.5 Cell Staining with Calcein AM and with CellTiter-Glo[®] Luminescent Kit for Assessing Membrane Integrity and Measuring Cellular ATP Levels

For cell staining, compound and DME-treated HEK 293 cells on the 384-pillar plate were rinsed once for 10 minutes by immersing the 384-pillar plate in a fresh

384-well plate containing 60 µL of a saline solution containing 140 mM NaCl and 20 mM $CaCl_2$. After discarding the 384-well plate with saline solution, the 384-pillar plate was sandwiched with a new 384-well plate containing 40 µL of 0.5 µM calcein AM (ThermoFisher) and incubated for 1 hour in the dark. After cell staining, excess calcein AM in the cell spots were removed by rinsing the 384-pillar plate with 60 µL of the saline solution for 10 minutes. To obtain fluorescent images of cell spots, the 384-pillar plate was sandwiched with a fresh 384-well plate with saline solution and scanned with the S+ Scanner (ATI, Republic of Korea), an automated epifluorescence microscope developed for rapid image acquisition at 15 frames per second (FPS). Green fluorescent cell images were obtained at 4X magnification with the Olympus UPLFLN 4X (numerical aperture (NA) 0.13, f-number 26.5, and depth of field (DOF) ~ 32.3 µm) (Olympus, Tokyo, Japan) and a green filter (XF404 from Omega Optical). ImageJ was used to extract fluorescent intensity from the images obtained.

Immediately after calcein AM staining and scanning, the cells on the 384-pillar plate were immersed in 40 µL of CellTiter-Glo® luminescent cell viability kit (Promega, Madison, WI, USA) in a 384-well plate to measure cellular ATP levels. To induce cell lysis, the sandwiched 384-pillar/well plates were shaken on an orbital shaker for 2 minutes. After stabilizing the luminescence for 10 minutes at room temperature, the luminescent signals were recorded using the plate reader at an emission wavelength of 560 nm. Overall experimental procedures are illustrated in Figure 6.
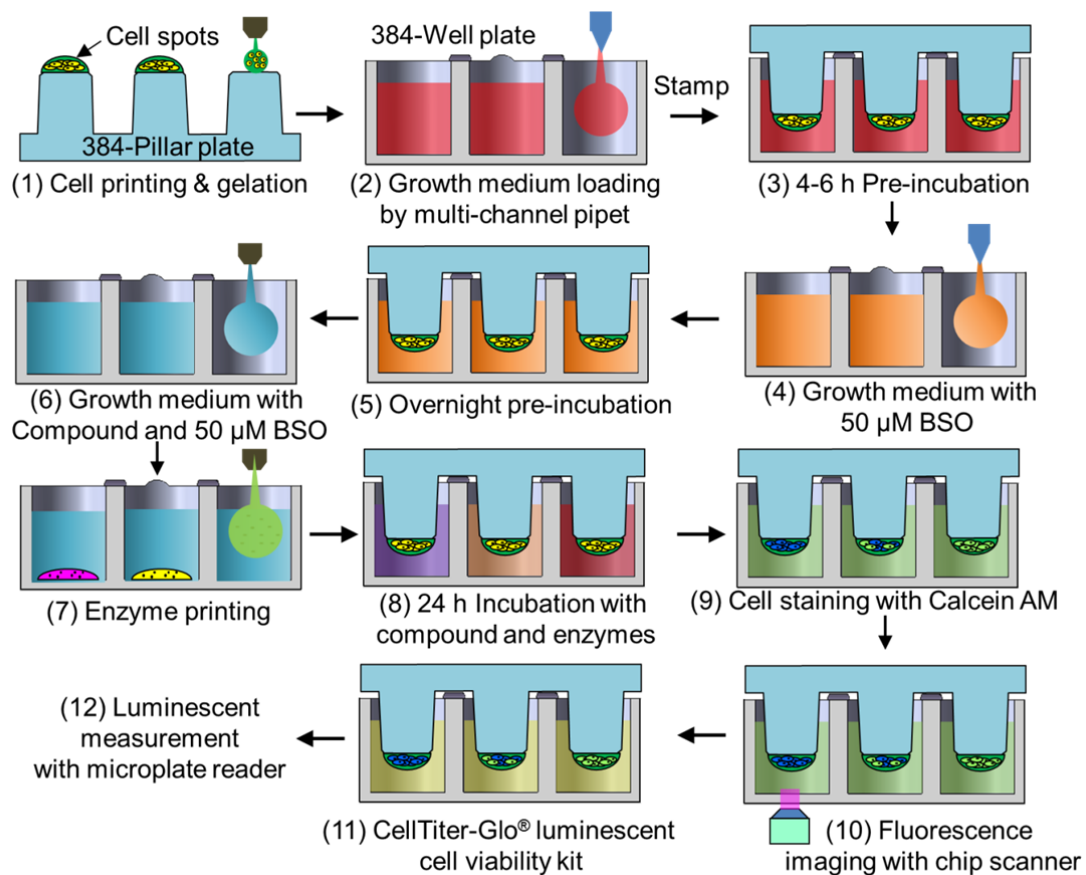
Figure 6. Schematic of experimental procedures for metabolism-induced toxicity assays

CHAPTER IV

IMAGE AND DATA ANALYSIS

4.1 Image Analysis

Since the background luminescence (or fluorescence) of completely dead HEK 293 cells (following treatment with 70% methanol for 1 h) was negligible due to background subtraction, the percentage of live HEK 293 cells was calculated using the following equation:

$$\% \textbf{ Live cells} = \left[\frac{\boldsymbol{F_{Reaction}}}{\boldsymbol{F_{Max}}}\right] \textbf{x } \textbf{100}$$

where $F_{Reaction}$ is the luminescence (or fluorescence) intensity of the reaction spot and F_{Max} is the luminescence (or fluorescence) intensity of fully viable cells.

To produce a conventional sigmoidal dose-response curve with response values normalized to span the range from 0% to 100% plotted against the logarithm of test concentration, we normalized the luminescence (or fluorescence) intensities of all cell spots with the luminescence (or fluorescence) intensity of a 100% live cell spot (a cell spots contacted with no compound) and converted the test compound concentration to their respective logarithms using Prism 4 (GraphPad Software, San Diego, CA). The sigmoidal dose-response curves (variable slope) and IC_{50} values (i.e., concentration of the compound where 50% of cell viability/growth inhibited) were

28

obtained using the following equation:

$$Y = Bottom + \left[\frac{Top - Bottom}{1 + 10^{(LogIC_{50}-X)\times H}}\right]$$

where IC_{50} is the midpoint of the curve, H is the hill slope, X is the logarithm of test concentration, and Y is the response (% live cells), starting from the top plateau (Top) of the sigmoidal curve to the bottom plateau (Bottom).

4.2 Calculation of the Coefficient of Variation (CV) and the Z' Factor

The CV is the ratio of the standard deviation (SD) to the average (Avg). It represents variability in relation to the average signal strength, thus the inverse of the signal-to-noise ratio [135].

$$CV = \frac{SD}{Avg} \times 100$$

To establish the robustness of the assays on the 384-pillar plate, the reproducibility and range of error were measured using the Z' factor and the coefficient of variation (CV). The Z' factor can be explained by the following equation:

$$Z' = \frac{(Avg_{Max} - 3SD_{Max}) - (Avg_{Min} + 3SD_{Min})}{Avg_{Max} - Avg_{Min}}$$

where Avg_{Max} is the average of all maximum luminescence intensity from fully viable HEK 293 cells on the 384-pillar plate, SD_{Max} is the standard deviation of maximum luminescence intensity, Avg_{Min} is the average of all minimum luminescence intensity from the dead cells affected by the highest dose of acetaminophen, and SD_{Min} is the standard deviation of minimum luminescence intensity.

4.3 Statistical Analysis of IC_{50} Values

Statistical analysis was performed with GraphPad Prism 4.0 to calculate IC_{50} values and standard errors obtained from triplicate 384-pillar plates, with each plate containing four replicates of each test condition. One-way analysis of variance (ANOVA) was used to compare the mean IC_{50} values of test compounds obtained from HEK 293 cells and individual DMEs. Statistically significant IC_{50} difference between no enzyme control and enzyme test conditions was indicated by * for $P < 0.05$ and ** for $P < 0.01$.

CHAPTER V

RESULTS AND ANALYSIS

5.1 Encapsulation of HEK 293 cells on the 384-pillar Plate and Measurement of DME Activity in the 384-well Plate

Prior to testing for metabolism-induced toxicity, robust surface chemistry was developed to prevent the detachment of HEK 293 cell spots from the surface of 384-pillars. In addition, the basal toxicity of DMEs originated from cryo-protectants added has been investigated. To minimize the basal toxicity issues, dilution ratios of DMEs in growth media and cell seeding density have been adjusted to maintain cell viability above 80% (data not shown). In general, a minimum of a 10-fold dilution of the stock 1000 nM DME was necessary for 1000 HEK 293 cells seeded per 384-pillar. For robust spot attachment and cell encapsulation, the 384-pillar plate (2 mm pillar diameter, 10.42 mm pillar height, and 4.5 mm pillar-to-pillar distance) was coated with 0.01% PMA-OD and then treated with 0.0033% PLL and 16.66 mM $BaCl_2$. The maleic anhydride groups within PMA-OD were used to covalently bond the amine groups within PLL . This surface chemistry application allowed negatively charged alginate to bind to positively charged PLL by ionic interaction. $BaCl_2$ was added to the PLL solution for the gelation of the alginate matrix. An array of 216 spots (1000 HEK 293 cells

31

entrapped in 1.5 μL of 0.75% alginate and 1 mg/mL Matrigel) were printed in 5 minutes using the microarray spotter. The alginate matrices with HEK 293 cells were found to be strongly attached to the surface of 384-pillars by the applied surface chemistry. Scanned images of the HEK 293 cells show that they had been suspended in 3D within the alginate matrix, indicating cell encapsulation was successful (Figure 7).
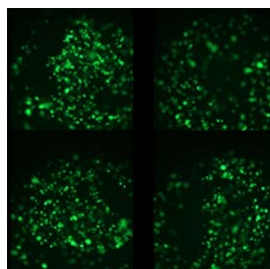
Figure 7. Enlarged images of calcein AM stained HEK 293 cells on the 384-pillar plate

Bio-printed HEK 293 cells on the 384-pillar plate were cultured in 3D by sandwiching with a 384-well plate containing DMEM supplemented with 10 % FBS, 1 % antibiotics, and BSO. BSO was used to increase the sensitivity of reactive metabolites generated by DMEs. After 24-hour pre-incubation, HEK 293 cells on the 384-pillar plate were exposed to nine test compounds combined with six representative DME conditions in a new 384-well plate. For example, representative Phase I DMEs, such as CYP1A2, CYP2B6, CYP2C9, CYP2D6, CYP2E1, and CYP3A4, and a Phase II DME, UGT1A4, have been used (Figure 6). Lee et al. demonstrated that encapsulated CYP450 isoforms in alginate, such as CYP1A2, CYP3A4, and CYP2D6, were highly active [136]. The activities of all DMEs used in this study were determined in 384-well plates prior to testing for metabolism-induced toxicity against HEK 293 cells with nine compounds. All enzymes tested were highly active in DMEM with the fluorescent substrates and cofactors (Figure 8 and Table 1).

(A)

BOMCC substrate

(B)

EOMCC substrate

(C)

**4-methylumbeliferone (4-MU)
(UGT1A4 activity)**
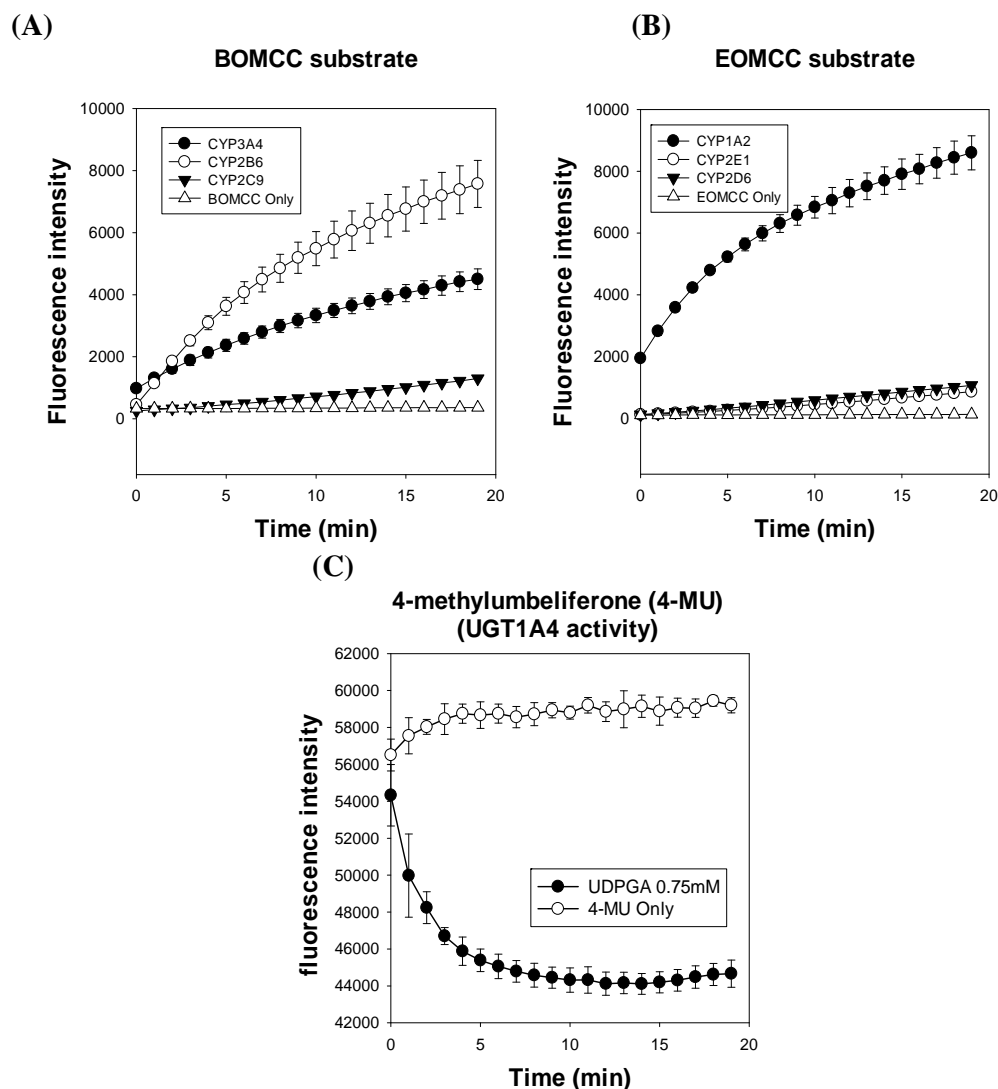
Figure 8. Enzyme activity determined with fluorogenic substrates. (A) BOMCC substrate. (B) EOMCC substrate (C) UGT1A4 activity was measured with 4-methylumbeliferone (4-MU). Fluorescence intensity decreased over time due to transfer of the glucuronic acid component of UDPGA to 4-MU *via* UGT1A4.

5.2 Robustness of the Assays Established on the 384-pillar Plate

For robust assay development on the 384-pillar plate, it is important to measure the range of errors and plate-to-plate and day-to-day reproducibility. The Z' factor and the coefficient of variation (CV) have been commonly calculated to evaluate the robustness and error ranges of an assay [135]. The robustness of the CellTiter-Glo® assay on the 384-pillar plate was determined by calculating Z' factors with acetaminophen incubated with CYP450 isoforms. The Z' factors calculated from

33

the 384-pillar plate were between 0.57 - 0.93 (Table 2). Since the acceptable range of the Z' factor is between 0.5 - 1 [135][137], we concluded that the CellTiter-Glo® luminance assay on the 384-pillar plate is robust and suitable for accurately identifying changes in compound toxicity by DMEs. In addition, the CV values were measured at three different dates to evaluate day-to-day variability of the CellTiter-Glo® assay. The data was collected from HEK 293 cells on the 384-pillar plate exposed to no compound and no enzyme. This method allowed us to calculate the CV values and understand variability of cell printing and day-to-day experimental variability (Figure 9). Our overall CV value of 13.8% indicates that the experimental errors are within acceptable ranges (typically below 20%) for HTS [135][137].

Table 2. Robustness of the CellTiter-Glo® assay tested with acetaminophen

Test conditions	Z' factor	IC$_{50}$ values (μM)
Control baculosome	0.75	125.7 ± 3.3
CYP1A2	0.63	79.1 ± 3.5
CYP2B6	0.57	77.1 ± 3.5
CYP2C9	0.79	66.3 ± 3.9
CYP2E1	0.69	62.5 ± 2.6
CYP3A4	0.93	89.2 ± 12.8
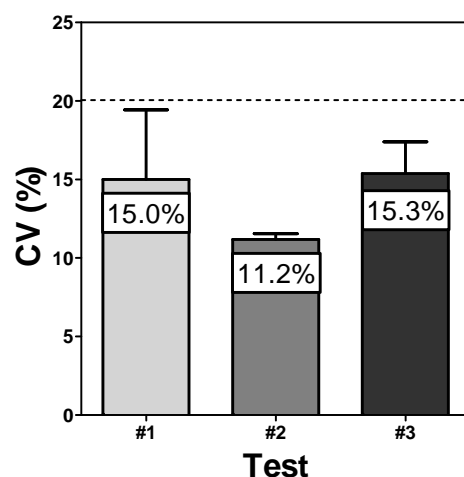
Figure 9. Variability of CellTiter-Glo® luminance intensities obtained from several 384-pillar plates prepared on different days

34

5.3 Dose Response Curves and IC$_{50}$ Values Obtained from Calcein AM Staining and the CellTiter-Glo® Luminescence Assay

Cell membrane integrity and cellular ATP levels in HEK 293 cells on the 384-pillar plate were assessed using calcein AM staining followed by a CellTiter-Glo® assay after 24-hour exposure to various concentrations of nine compounds, five DMEs, and one no enzyme control. Each assay was performed with nine dosages (1.95 μM – 250 μM) in four replicates, resulting in 1944 data points (i.e., 9 compounds x 6 enzyme conditions x 9 dosages x 4 replicates). The percent of HEK 293 cells viable after 24-hour exposure to various concentrations of test compounds and five DMEs at different dosages were compared with those of 100% viable cells exposed to no compounds (DMSO alone control) to calculate IC$_{50}$ values. We marked IC$_{50}$ values showing more than a 50% difference with the control as a meaningful indication of metabolism-induced effects, where red-marked IC$_{50}$ values indicate compound toxicity is enhanced (augmented toxicity) due to DMEs added and blue-marked IC$_{50}$ values indicate compound toxicity is reduced (detoxification) in the presence of DMEs. Black-marked IC$_{50}$ values indicate no changes in compound toxicity in the presence of DMEs. Calcein AM, which is a fluorogenic compound, can be transported through the cellular membrane and produce a green fluorescent signal when the cell membrane is intact, making it useful for cell viability assessment [138]. However, it tends to be less sensitive compared to other viability endpoints, such as mitochondrial membrane potential with tetramethyl rhodamine methyl ester or ATP level measurement with the CellTiter-Glo® assay [139]. This cell viability assay, which uses ATP amount detection in the cell, is the fastest and most sensitive assay and has less artifacts than other cell viability assay methods [140].

35

We also observed relatively higher IC_{50} values with calcein AM staining, presumably due to cell staining immediately after 24-hour incubation with compounds and DMEs. Nonetheless, benzo[a]pyrene, cyclophosphamide, 2-naphthlyamine, and 6-aminochrysene clearly showed augmented toxicity on multiple CYP450 isoforms (Table 3). For example, 2-naphthlyamine incubated with CYP2E1, CYP2B6, CYP1A2, and CYP3A4 induced striking decreases in HEK 293 cell viability (Figure 10). The dose response curves and the IC_{50} values of the nine compounds and their potential DME-generated metabolites are summarized in Table 3 and Figure 11 for calcein AM staining.

Table 3. IC_{50} values of compounds tested with the calcein AM assay on the 384-pillar/well plates

Compounds	No enzyme	CYP 3A4	CYP 1A2	CYP 2B6	CYP 2C9	CYP 2D6	CYP 2E1	UGT 1A4
Benzo[a]pyrene	>250	>250	194 ± 9.8***	>250	-	-	>250	>250
Aflatoxin B1	>250	>250	>250	>250	-		>250	>250
Cyclophosphamide	>250	241 ± 14.6	-	>250	>250	-	>250	>250
2-Naphthlyamine	>250	163 ± 35.6**	151 ±13.8***	247 ± 14.3	-	-	90 ±21.9***	>250
Acrylamide	>250	>250	-	>250	>250	-	>250	>250
Doxorubicin HCl	>250	241 ± 19.0	-	>250	-	>250	-	>250
6-Aminochrysene	>250	80.3 ± 0.9***	>250	103 ± 50***	-	-	>250	>250
8-Methoxypsoralen	>250	>250	>250	-	>250	-	>250	>250
4-Nitrophenol	>250	>250	>250	-	>250	-	>250	>250

- To determine statistically significant IC_{50} differences between no enzyme control and enzyme test conditions, one-way ANOVA analysis was performed and the results were indicated as ** for $p < 0.01$ and *** for $p < 0.0001$. No indication means $p > 0.05$.
- Red highlighted IC_{50} values indicate augmented toxicity.
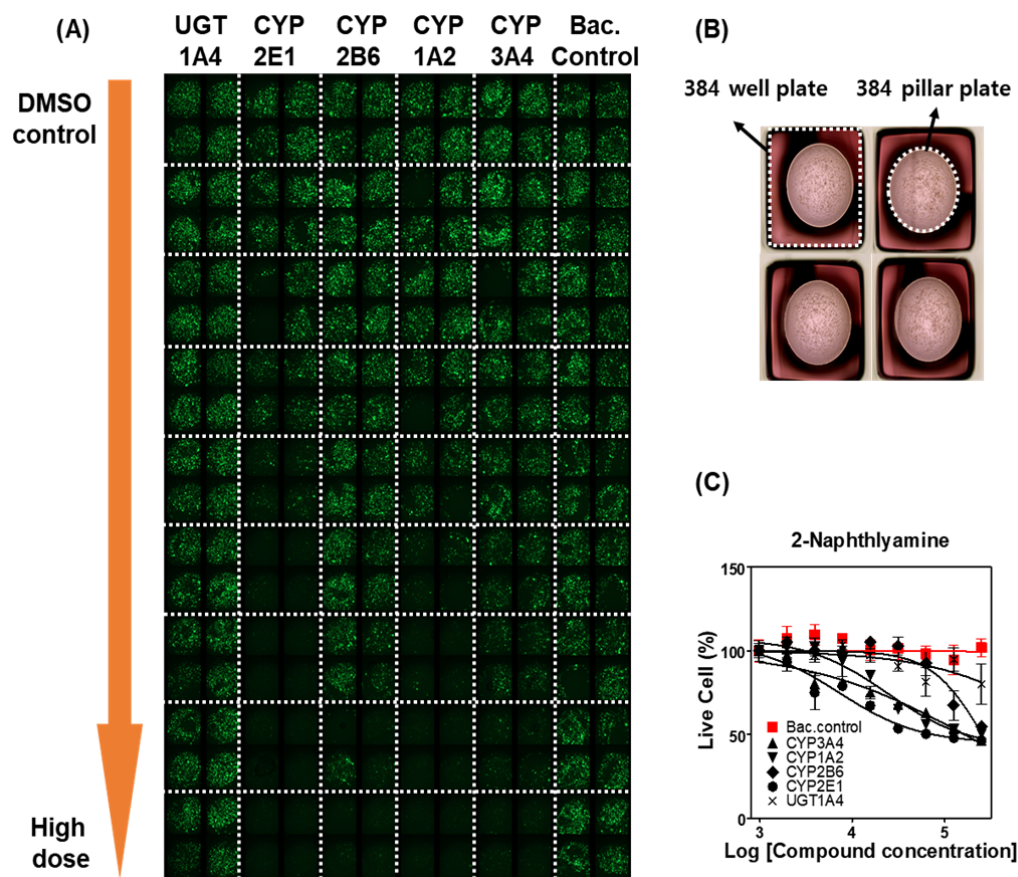
Figure 10. Metabolism-induced toxicity assays with HEK 293 cells on the 384-pillar plate and drug-metabolizing enzymes (DMEs) and 2-naphtylamine in the 384-well plate: (A) Scanned images of HEK 293 cells on the 384-pillar plate (B) Microscopic images of the 384-pillar plate with HEK 293 cells sandwiched with the 384-well plate containing 2-naphtylamine and DMEs. The white dotted square represents the 384-well and the white dotted circle indicates the 384-pillar. (C) Dose response curves obtained from the green fluorescent images on the 384-pillar plate.
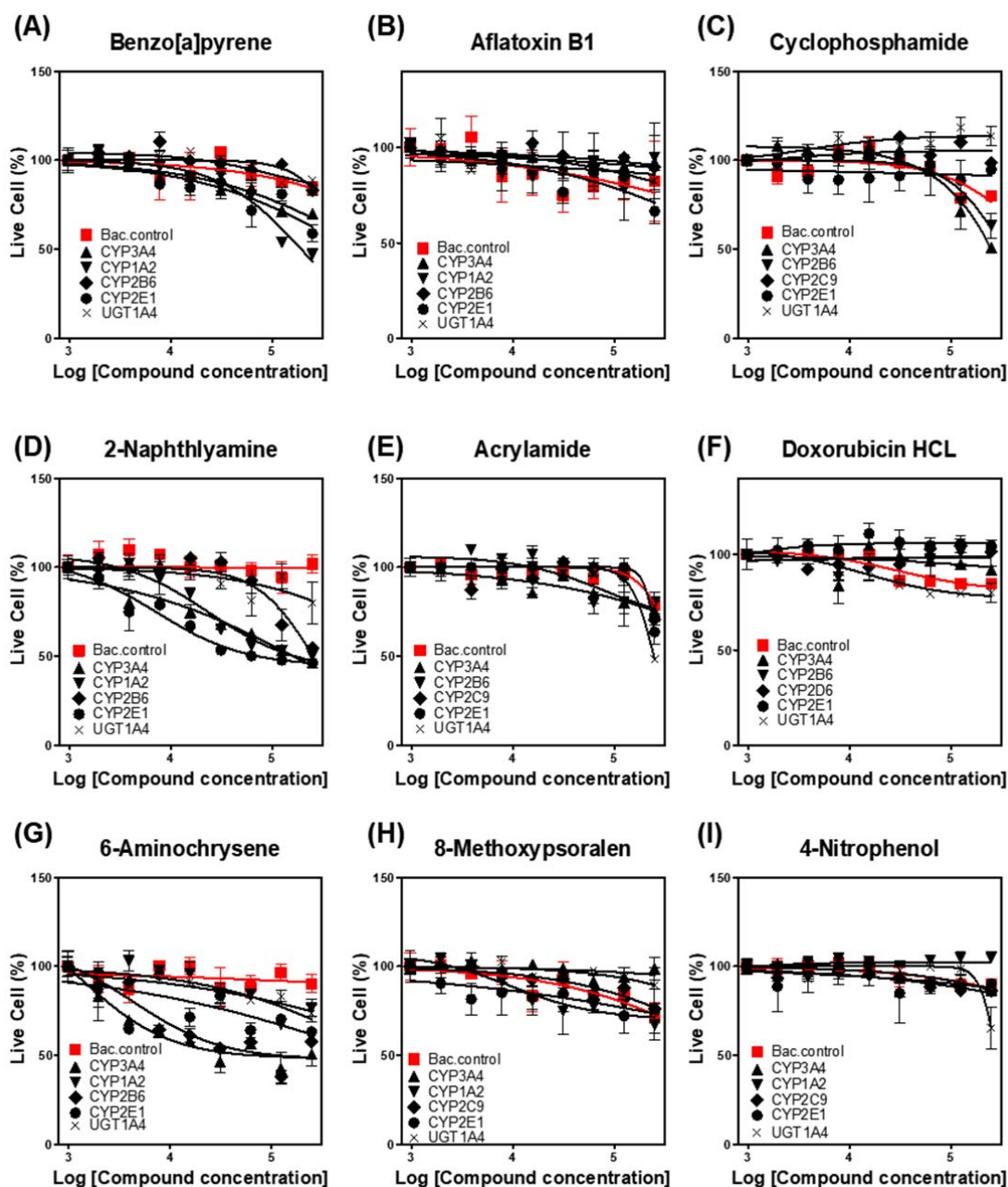
Figure 11. Dose response curves of compounds tested with the calcein AM assay on the 384-pillar/well plates.

Additionally, ATP levels within HEK 293 cells in the presence and absence of DMEs have been quantified as an indicator of metabolically active cells using the CellTiter-Glo® luminescence assay [140]. As expected, we observed relatively lower IC_{50} values with the CellTiter-Glo® luminescence assay (Table 4). Six compounds out

of nine demonstrated metabolism-induced augmented toxicity. Benzo[a]pyrene, cyclophosphamide, 2-naphthylamine, doxorubicin, 6-aminochrysene, and 8-methoxypsoralen demonstrated augmented toxicity on either P450 isoforms or UGT1A4. In particular, the 2-naphthlyamine, 6-aminochrysene, cyclophosphamide, and 8-methoxypsolarentest conditions decreased more than 10-fold when added with CYP450s, compared to Baculosome controls (Figure 12 and Figure 13). Unlike other compounds, acrylamide was detoxified in the presence of UGT1A4 (Table 4). This can be explained by metabolites of Phase I DMEs *in vivo* being conjugated by Phase II DMEs, including UGTs, SULTs, and GSTs, leading to detoxification and rapid excretion [141]. Two compounds, aflatoxin B1 and 4-nitrophenol, were nontoxic at given dosages regardless of DMEs added.

Table 4. IC$_{50}$ values of compounds tested with the CellTiter-Glo® assay on the 384-pillar/well plates.

Compounds	No enzyme	CYP 3A4	CYP 1A2	CYP 2B6	CYP 2C9	CYP 2D6	CYP 2E1	UGT 1A4
Benzo[a]pyrene	>250	229 ± 12.8	245 ± 18.2	116 ± 7.8***	-	-	233 ± 9.1	>250
Aflatoxin B1	>250	>250	>250	>250	-	-	>250	>250
Cyclophosphamide	>250	66 ±18.3***	-	155 ± 5.8***	>250		>250	>250
2-Naphthlyamine	>250	25 ± 3.6***	20 ± 3.3***	56 ± 22.5***	-	-	24 ± 1.4***	179 ± 36.9**
Acrylamide	186 ± 10.1	164 ± 23.5	-	165 ± 25.6	208 ± 3.3	-	188 ± 36.2	246 ± 46.9
Doxorubicin HCl	74 ± 0.7	25 ± 0.7***	-	12 ± 3.2***	-	10 ± 2.1***	11 ± 1.1***	42 ± 1.7***
6-Aminochrysene	93 ± 10.7	9 ± 3.0***	32 ± 7.1***	9 ± 1.7***	-	-	19 ± 2.4***	26 ± 12.3***
8-Methoxypsoralen	>250	>250	126*** ± 41.1	-	>250	-	213 ± 33	>250
4-Nitrophenol	>250	>250	>250	-	>250	-	>250	>250

- To determine statistically significant IC$_{50}$ differences between no enzyme control and enzyme test conditions, one-way ANOVA analysis was performed and the results were indicated as ** for $p < 0.01$ and *** for $p < 0.0001$. No indication means $p > 0.05$.

- Red highlighted IC$_{50}$ values indicate augmented toxicity whereas blue highlighted IC$_{50}$ value indicates detoxification.
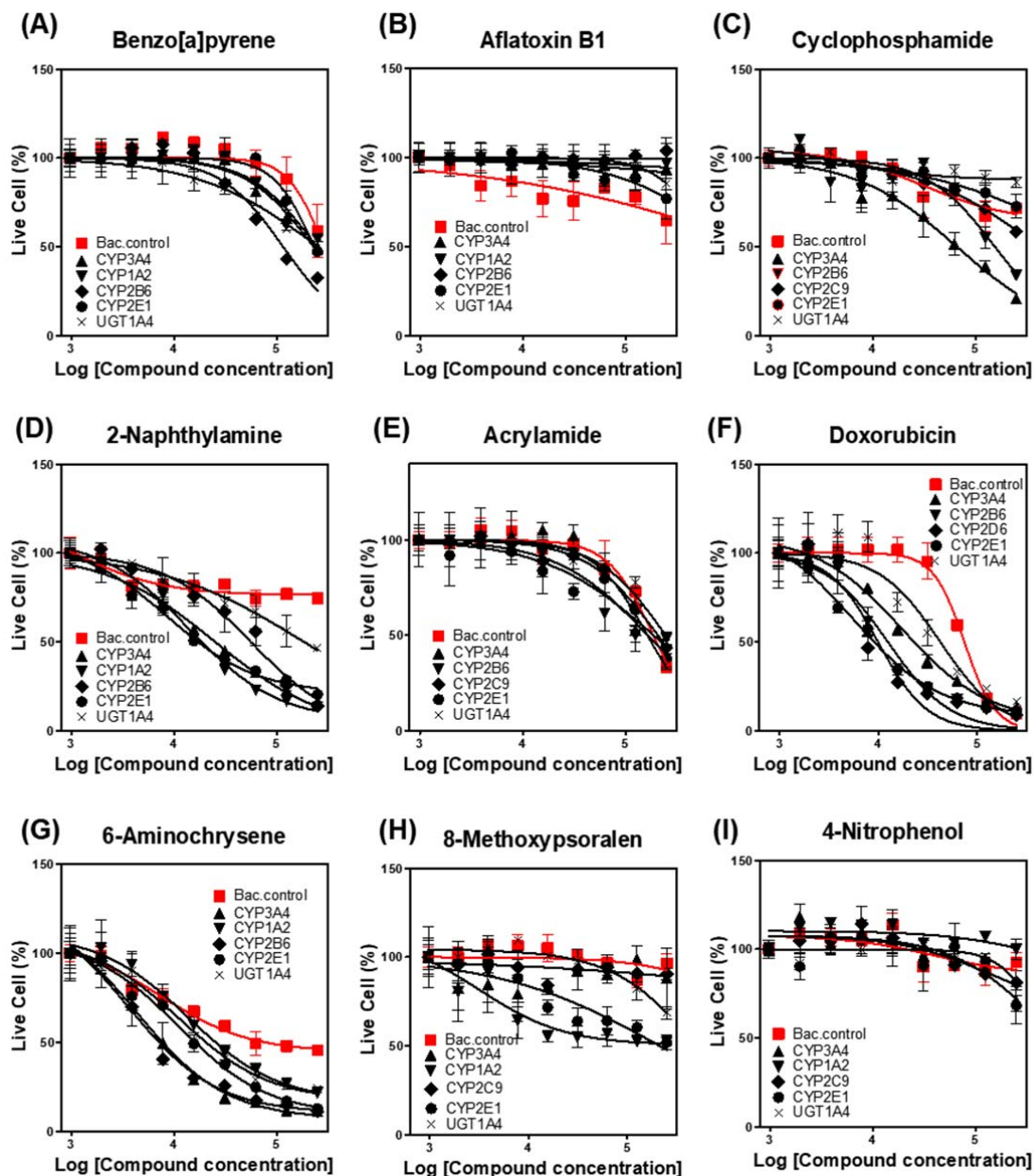
Figure 12. Dose response curves of compounds tested with the CellTiter-Glo® assay on the 384-pillar/well plates.
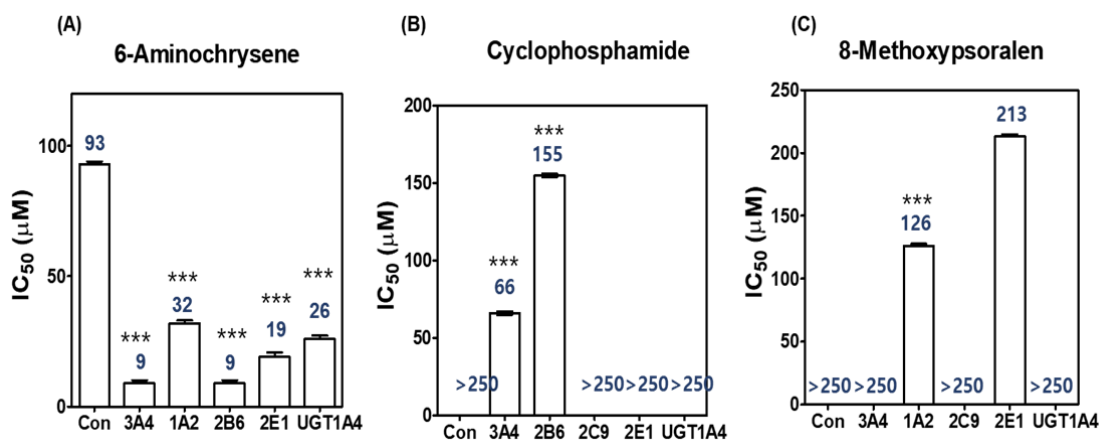
Figure 13. Representative IC$_{50}$ values showing strong responses when CYP450 isoforms added.

- To determine statistically significant IC$_{50}$ differences between no enzyme control and enzyme test conditions, one-way ANOVA analysis was performed and the results were indicated as *** for $p < 0.0001$. No indication means $p > 0.05$.

  To verify that our metabolism toxicity assay with the 384-pillar platform was accurate, the results were compared with literature. For example, cyclophosphamide, which has been widely used for chemotherapy, is also known to have severe side-effects and toxicities to humans. The main active metabolite of cyclophosphamide, 4-hydroxycyclophosphamide, is metabolized by cytochrome P450 (CYP450) isoforms, such as CYP3A4 and CYP2B6, which directly affects cytotoxic mechanisms [142] [143]. In our result, the 384-pillar platform was able to identify that CYP3A4 and CYP2B6 strongly activated cellular toxicity by the conversion of cyclophosphamide to its cytotoxic metabolite. In addition, 2-naphthlyamine is known to be a human carcinogen based on its metabolites, including N-hydroxylamine, which is formed by CYP450 isoforms, such as CYP3A4, CYP2E1, and CYP1A2, as well as UGT1A4. The metabolites undergo a number of conjugation reactions forming additional functional groups [100-103]. On the 384-pillar platform, 2-naphthlyamine was shown to be converted to its cytotoxic metabolites by CYP3A4, CYP1A2, CYP2B6,

CYP2E1, and UGT1A4. 2-Naphthlyamine was particularly susceptible to reactions with CYP3A4, CYP1A2, and CYP2E1. In addition, other compounds and their partnered DME reaction toxicities were compared to literature and found to be congruent (Table 5). From these results, we concluded that the 384-pillar platform has the capacity as an alternative *in vitro* test platform for *in vivo* metabolite toxicity testing.

Table 5. Drug metabolizing enzymes (DMEs) involved in metabolism of the compounds.

Compounds	DMEs identified from this study	Known DMEs in literature	References
Benzo[a]pyrene	CYP1A2, CYP2B6, CYP2C9, CYP3A4	CYP1A2, CYP2C9, CYP3A4	Luckert et al.,2013 Yun et al., 1992 Bauer et al., 1995
Aflatoxin B1	-	CYP1A2, CYP3A4	Dohnal et al., 2014 Guengerich et al., 1992
Cyclophosphamide monohydrate	CYP2B6, CYP3A4	CYP2B6, CYP2C9, CYP3A4	Chang et al., 1993 Huang et al., 2000
2-Naphthylamine	CYP1A2, CYP2B6, CYP2E1, CYP3A4, UGT1A4	UGT family	Kadlubar et al., 1977 Pacifici et al., 1986
Acrylamide	UGT1A4	CYP2E1	Settels et al., 2008
Doxorubicin HCL	CYP2B6, CYP2D6, CYP2E1, CYP3A4, UGT1A4	Aldo-keto reductase	Speth et al., 1988 Minotti et al., 2001
6-Aminochrysene	CYP1A2, CYP2B6, CYP2E1, CYP3A4, UGT1A4	CYP1A2, CYP2B6, CYP3A4	Kadlubar et al., 1987 Shimada et al., 1989
8-Methoxypsoralen	CYP1A2	CYP1A2, CYP2E1	Deeni et al., 2013
4-Nitrophenol	-	CYP2E1, CYP3A	Zerilli et al., 1997

CHAPTER VI

DISCUSSION AND CONCLUSIONS

There have been tremendous efforts made by regulatory agencies in the world to better predict toxicity of chemicals in humans using *in vitro* and *in silico* methods and to reduce the use of animals in toxicity assessment. In response to this need, our group has been developing several microarray biochip platforms to predict metabolism-induced compound toxicity in humans: the MetaChip [12], the DataChip [13][135][144] and the TeamChip [14]. Although these biochip platforms are ideally suited for miniaturized 3D cell cultures by bioprinting and rapid testing compound metabolism, their footprint is too small for commonly used robotic dispensing systems and cell imaging systems in HTS assays. To resolve these compatibility issues, we have developed a 384-pillar plate, which can be combined with 384-well plates for 3D cell cultures and compound toxicity testing. In addition, cell images and absorbance, fluorescence, and luminescence signals from cells can be easily obtained from HCI imagers and microtiter plate readers. With this technology and platform, we participated in Stages I and II of the Transform Tox Testing Challenge. The scope of the challenge was to test the nine model compounds against HEK 293 cells and rapidly identify metabolism-mediated toxicity. To address the scope of the work and predict metabolism-induced toxicity, we printed HEK 293 cells in an alginate-Matrigel mixture on the 384-pillar plate, which was sandwiched into

the 384-well plate containing combinations of compounds and DMEs. Our results indicate that the toxicity of 78% of the test compounds were significantly changed when DMEs were incorporated. Our 384-pillar plate offers several advantages over more conventional 2D and 3D cell culture models (Table 6), thus providing rapid generation of human organotypic cell cultures for compound screening and superior data quality and predictive outcomes of drug candidates' effects *in vivo*. The 384-pillar plate requires relatively small amounts of cells and hydrogels (typically 1 - 2 μL) for creating and evaluating bioprinted 3D cells. Cell encapsulation protocols developed are flexible and allow for culturing multiple cell types from different organs in hydrogels on the 384-pillar plate, consequently providing more insight into potential organ-specific toxicity of compounds. Miniaturized 3D cell cultures on the 384-pillar plate may serve as disease models to provide a microenvironment that simulates specific biochemical functions and morphological features of human tissues found *in vivo*. The 384-pillar plate is compatible with standard 384-well plates and existing HTS equipment. Highly reproducible, high-throughput precision printing allows us to test a variety of cell culture conditions and drugs in combination, which makes it well suited for early stage HTS of compound libraries. Cell image acquisition from miniaturized 3D cell cultures is easy and straightforward because the whole sample depth fits within the focus depth of a normal objective (typically 2 x or 4 x magnification). High-throughput, HCI on miniaturized 3D cell cultures can decipher toxicodynamic and toxicokinetic traits of drugs and provide more insight into complicated toxicology pathways and related adverse responses in early stages of drug discovery. This unique feature of the 384-pillar plate provides the capability to test the effects of multiple DMEs against 3D-cultured cells for metabolism-induced compound toxicity. This predictive information on toxicity will be extremely valuable

to minimize adverse drug responses for new and existing drugs. Thus, our approach may potentially lead to increased drug research success rates by enabling more effective and safer compounds to enter preclinical evaluations and clinical trials.

Table 6. Advantages of using the 384-pillar plate platform for metabolism-induced toxicity.

Advantages	Future directions
Miniaturized 3D cell culture	Perform co-culture or layered cell culture to better mimic tissue structures *in vivo*
High-throughput metabolism-induced assays	Incorporate other organ cell types to mimic effects of drug metabolism in multi-organ systems (e.g., 3D-cultured primary hepatocytes on the 384-pillar plate coupled with brain cells in the 384-well plate)
Robust and straightforward protocols for high-throughput compound screening	Further improve the CV and the Z' factor for printing colloidal samples with improved micro-solenoid valves
Highly flexible and mechanistic toxicity assays	Include additional high-content cell staining for elucidating mechanisms of drug-induced toxicity
Rapid 3D cell imaging due to small dimensions	Test image acquisition with conventional high-content imagers and further develop software for rapid 3D cell image processing
High predictivity of hepatotoxicity *in vivo*	Analyze the data obtained from the 384-pillar plate with *in vitro–in vivo* correlation (IVIVC) models
Cost effectiveness	Further miniaturize the assays on a higher density pillar plate

Like all other *in vitro* alternative models, our current approach to predict metabolism-induced toxicity in high throughput faces several technical challenges (Table 6). One of the biggest challenges is instability of commercially available DMEs. Most DMEs lose their metabolic capability within 24 hours, leading to insufficient biotransformation of test compounds. This could potentially be an issue to identify metabolism-induced toxicity of slow-metabolizing compounds. Indeed, we have observed no response on DMEs for aflatoxin B1 and 4-nitrophenol presumably due to these reasons. In addition, it is difficult to test all DMEs expressed in primary hepatocytes on the 384-pillar plate platform, although the platform is still better suited for testing mechanistic pathways of drug metabolism. There are several other

technical challenges, including drug diffusion, contamination of commercially available DMEs, and basal toxicity of DMEs. However, there is plenty of room for improvement to further perfect the technology (Table 7).

Table 7. Current challenges of the 384-pillar plate platform for metabolism-induced toxicity and potential solutions.

Challenges	Causes	Potential solutions
Insufficient biotransformation	DME stability is low (i.e., half-life is about 2 hours for P450s)	Enhance DME stability by immobilization of the enzymes on lipid membranes or supplementation with cofactors (e.g., cytochrome b5)
	It may lack specific enzymes necessary for drug metabolism	Use encapsulated primary hepatocytes and HepaRG cells instead of DMEs to provide metabolism competence
Metabolite diffusion into cells	Hydrophilic metabolites generated outside cells may not penetrate cell membranes	Use hepatic cells expressing DMEs (e.g., TeamChip, primary hepatocytes, and HepaRG cells)
Differential cellular responses by metabolites	Metabolites generated may not rupture cell membranes or inhibit cell growth	Measure other indicators of hepatotoxicity (e.g., mitochondrial damage, apoptosis, steatosis, phospholipidosis, etc.)
Contamination	Commercially available DMEs are often contaminated with microbials	Test contamination of commercial DMEs prior to use, or produce DMEs in sterile conditions
Basal toxicity of DMEs	Additives (e.g., cryoprotectants) in DME solutions are cytotoxic	Dilute DME solutions at least 10-fold or produce DMEs in-house with less toxic additives

We have successfully completed Stages I and II of the TTTC with the 384-pillar plate and cell printing technology and demonstrated metabolism-induced toxicity of compounds. The 384-pillar plate is a high-throughput, cost-efficient platform for determining the cytotoxicity of compounds and their metabolites. It is highly flexible for 3D cell cultures and can be tailored to include any combination of DMEs to investigate potential individual metabolic profiles. Although we only demonstrated encapsulation of HEK 293 cells on the 384-pillar plate, the cell printing and encapsulation technology can be easily extended to include a variety of different human cell types to assess organ-specific toxicity. In addition, calcein AM and

CellTiter-Glo® luminescent cell viability assays demonstrated on the 384-pillar plate can be extended to include other HCI assays to better predict hepatotoxicity of compounds. Changing growth media over time for 3D cell cultures and cell imaging on the 384-pillar plate are straightforward and convenient, allowing users to monitor changes in various cell signals *in situ* using HCI imagers and microtiter plate readers. Therefore, we envision that the 384-pillar plate platform can serve as a promising high-throughput, 3D-cell based, *in vitro* assay tool for predictive human toxicology.

CHAPTER VII

FUTURE WORK

1. Sufficient Biotransformation

Commercial DMEs lose their stability within 2 hours. To give enough biotransformation, adding encapsulated HepaRG cells or inserting cofactors such as cytochrome b5 will increase the metabolism competence.

2. Wide range of high-content assays

We have successfully proved that the 384-pillar plate can be used to understand metabolism-mediated toxicity. However, we only used two endpoints related to cell viability. High-content imaging (HCI) assays are capable of quantifying several cellular responses. Further expansion of HCI assays on the 384-pillar platform is necessary, which will be a great benefit to understand multi-parametric mechanistic toxicity. This effort will help us analyze multiple endpoints of environmental chemicals such as target specific signals like mitochondrial dysfunction, DNA impairment, and apoptosis/necrosis.

REFERENCES

[1]   May JE, Xu J, Morse HR, Avent ND, Donaldson C (2009) Toxicity testing: the search for an in vitro alternative to animal testing. Br J Biomed Sci 66(3):160-165

[2]   Lee MY, Dordick JS (2006) High-throughput human metabolism and toxicity analysis.   Curr   Opin   Biotechnol   17(6):619-627. doi:10.1016/j.copbio.2006.09.003

[3]   Roth AD, Lee MY (2017) Idiosyncratic Drug-Induced Liver Injury (IDILI): Potential Mechanisms and Predictive Assays. Biomed Res Int. 2017:9176937. doi: 10.1155/2017/9176937

[4]   Liebler DC, Guengerich FP (2005) Elucidating mechanisms of drug-induced toxicity. Nat Rev Drug Discov 4(5):410-420. doi:10.1038/nrd1720

[5]   Zamek-Gliszczynski MJ, Hoffmaster KA, Nezasa K-I, Tallman MN, Brouwer KLR(2006) Integration of hepatic drug transporters and phase II metabolizing enzymes: Mechanisms of hepatic excretion of sulfate, glucuronide, and glutathione   metabolites.   Eur   J   Pharm   Sci   27(5):447-486. doi:10.1016/j.ejps.2005.12.007

[6]   Cook D, Brown D, Alexander R, March R, Morgan P, Satterthwalite G, Pangalos MN (2014) Lessons learned from the fate of AstraZeneca's drug pipeline: a five- dimensional framework. Nat Rev Drug Discov 13(6):419-431. doi:10.1038/nrd4309

[7]   Tang C, Lin JH, Lu AYH (2005) Metabolism-based drug-drug interactions: What determines individual variability in cytochrome P450 induction? Drug Metab Dispos 33(5):603-613. doi:10.1124/dmd.104.003236

[8]   Karmaus AL, Filer DL, Martin MT, Houck KA (2016) Evaluation of food-relevant chemicals in the ToxCast high-throughput screening program. Food Chem Toxicol 92:188-196. doi: 10.1016/j.fct.2016.04.012

[9]   Richard AM, Judson RS, Houck KA, Grulke CM, Volarath P, Thillainadarajah I, Yang C, Rathman J, Martin MT, Wambaugh JF, Knudsen TB, Kancherla J, Mansouri K, Patlewicz G, Williams AJ, Little SB, Crofton KM, Thomas RS (2016) ToxCast Chemical Landscape: Paving the Road to 21st Century Toxicology.   Chem   Res   Toxicol   29(8):1225-1251.   doi: 10.1021/acs.chemrestox.6b00135.

[10]   Kienzler A., Halder M and Worth A (2017) Waiving chronic fish tests: possible use of acute-to-chronic relationships and interspecies correlations. Toxicological and Environmental Chemistry

[11]   Monamy, V. (2017). Animal experimentation: A guide to the issues. Cambridge University Press.

[12]   Lee MY, Park CB, Dordick JS, Clark DS (2005) Metabolizing enzyme toxicology assay chip (MetaChip) for high-throughput microscale toxicity analyses. Proc Natl Acad Sci 102(4):983-987. doi:10.1073/pnas.0406755102

[13]   Lee MY, Kumar RA, Sukumaran SM, Hogg MG, Clark DS, Dordick JS (2008) Three-dimensional cellular microarray for high-throughput toxicology assays. Proc Natl Acad Sci 105(1):59-63. doi:10.1073/pnas.0708756105

[14]   Kwon SJ, Lee DW, Shah DA, Ku B, Jeon SY, Solanki K, Ryan JD, Clark DS, Dordick JS, Lee MY (2014) High-throughput and combinatorial gene expression on a chip for metabolism-induced toxicology screening. Nat Commun 5:3739. doi: 10.1038/ncomms4739

[15] Chhabra RS, Bucher JR, Wolfe M, Portier C. 2003. Toxicity characterization of environmental chemicals by the US National Toxicology Program: an overview. Int J Hyg Environ Health 206:437–45

[16] Zurlo, J. et al. (1993) Animals and Alternatives in Testing: History, Science, and Ethics. Mary Ann Liebert, Inc.

[17] Tweats DJ, Scott AD, Westmoreland C, Carmichael PL. 2007. Determination of genetic toxicity and potential carcinogenicity in vitro - challenges post the Seventh Amendment to the European Cosmetics Directive. Mutagenesis 22:5–13.

[18] Williams, G. and Weisburger, G. (1993) Chemical carcinogenesis. In Toxicology.   The Basic Science of Poisons. McGraw-Hill

[19] National Toxicology Program, (2004) A National Toxicology Program for the 21st Century: A Roadmap for the Future

[20] David J, Dix, Keith A. Houck, The ToxCast Program for Prioritizing Toxicity Testing of Environmental Chemicals, Toxicological Sciences, Volume 95, Issue 1, 1 January 2007, Pages 5–12, https://doi.org/10.1093/toxsci/kfl103

[21] Judson,R.S; Houck, K.A.; Kavlock, R.J.; Knudsen, T. B.; Martin, M. T.; Mortensen, H. M., Reif, D. M.; Rotroff, D. M.; Shah, I.; Richard, A. M.; et al. In Vitro Screening of Environmental Chemicals for Targeted Testing Prioritization: The ToxCast Project. Environ. Health Perspect. 2010, 118(4), 485-492

[22] William P. Janzen and C. Nicholas Hodge, A Chemogenomic Approach to Discovering Target-Selective Drugs, Chem Biol Drug Des 2006; 67: 85–86

[23] Xia, M. et al. (2008) Compound cytotoxicity profiling using quantitative high throughput screening. Environ. Health Perspect. 116, 284–291

[24] Sunita J. Shukla, Ruili Huang, Christopher P. Austin and Menghang Xia, Foundation review: The future of toxicity testing: a focus on in vitro methods using a quantitative high-throughput screening platform, Drug Discovery Today, Volume 15, Numbers 23/24, December 2010

[25] Martin, M. T.; Dix, D.J.; Judson, R. S.; Kavlock, R.J.; Reif, D. M.; Richard, A. M.; Rotroff, D.M.; Romanov, S.; Medvedev, A.; Poltoratskaya, N.; et al. Impact of Environmental Chemicals on Key Transcription Regulators and Correlation to Toxicity End Points within EPA's Toxcast Program. Chem. Res. Toxicol. 2010, 23(3),578-590

[26] Valerio LG Jr. In silico toxicology for the pharmaceutical sciences. Toxicol Appl Pharmacol 2009, 241:356–370.

[27] Susan M. Pond, Thomas N. Tozer. First-Pass Elimination Basic Concepts and Clinical Consequences Clinical Pharmacokinetics, February 1984, Volume 9, Issue 1, pp 1–25

[28] Furge LL, Guengerich FP "Cytochrome P450 enzymes in drug metabolism and chemical toxicology: an introduction." Biochem Mol Biol Educ 2006, 34:66-74.

[29] Guengerich, F. P. "Cytochrome P450s and other enzymes in drug metabolism and toxicity." AAPS J. 8, E101–E111 (2006).

[30] Masuhiro, N. and Shinsaku, N. "Tissue-Specific mRNA Expression Profiles of Human Phase I Metabolizing Enzymes Except for Cytochrome P450 and Phase II Metabolizing Enzymes" Drug Metab, Pharmacokinet, 21 (5): 357-374 (2006).

[31] Kapitulnik, J. and Strobel, H. W.: Extrahepatic drug metabolizing enzymes. J. Biochem. Mol. Toxicol., 13: 227-230 (1999).

[32] Nishimura, M., Yaguti, H., Yoshitsugu, H., Naito, S. and Satoh, T.: Tissue distribution of mRNA expression of human cytochrome P450 isoforms

assessed by high-sensitivity real-time reverse transcription PCR. Yakugaku Zasshi, 12: 369-375 (2003).

[33] Urs A. Meyer "Overview of Enzymes of Drug Metabolism" Journal of Pharmacokinetics and Biopharmaceutics, Vol 24, No. 5, 1996

[34] Walgren JL, Mitchell MD, Thompson DC: Role of metabolism in drug-induced idiosyncratic hepatotoxicity. Crit Rev Toxicol 2005, 35:325-361.

[35] Scripture CD, Figg WD: Drug interactions in cancer therapy. Nat Rev Cancer 2006, 6:546-558.

[36] Tang C, Lin JH, Lu AYH: Metabolism-based drug-drug interactions: what determines individual variability in cytochrome P450 induction? Drug Metab Dispos 2005, 33:603-613.

[37] M. Ingelman-Sundberg, Human drug metabolising cytochrome P450 enzymes: properties and polymorphisms, Naunyn-Schmiedeberg's Arch Pharmacol (2004) 369 : 89–104

[38] F. P. Guengerich (2003) Cytochrome P450s, drugs, and diseases, Mol. Intervent. 3, 8–18.

[39] Wienkers, L. C., and Heath, T. G. (2005) Predicting in vivo drug interactions from in vitro drug discovery data. Nat. Rev. Drug Discovery 4, 825−833.

[40] Guengerich, F. P. (2005) Human cytochrome P450 enzymes. In Cytochrome P450: Structure, Mechanism, and Biochhemistry, 3rd ed. (Ortiz de Montellano, P. R., Ed.) pp 377−530, Kluwer Academic- Plenum Press, New York.

[41] Guengerich FP. Cytochrome P450 oxidations in the generation of reactive electrophiles: epoxidations and related reactions. Arch Biochem Biophys . 2003 ; 409 : 59 - 71 .

[42] Guengerich, F. P. (1977) Separation and purification of multiple forms of microsomal cytochrome P-450. Activities of different forms of cytochrome P-450 towards several compounds of environmental interest. J. Biol. Chem. 252, 3970−3979.

[43] Zamek-Gliszczynski MJ, Hoffmaster KA, Nezasa K, Tallman MN, Brouwer KLR: Integration of hepatic drug transporters and phase II metabolizing enzymes: mechanisms of hepatic excretion of sulfate, glucuronide, and glutathione metabolites. Eur J Pharm Sci 2006, 27:447-486.

[44] Lerche-Langrand C, Toutain HJ. Precision-cut liver slices: characteristics and use for in vitro pharmaco-toxicology. Toxicology. 2000; 153:221–253. [PubMed: 11090959]

[45] Hashemi E, Till C, Ioannides C. Stability of Phase II Conjugation Systems in Cultured Precisioncut Rat Hepatic Slices. Toxicol In Vitro. 1999; 13:459–466. [PubMed: 20654503]

[46] Ghantous HN, Fernando J, Gandolfi AJ, Brendel K. Sevoflurane is biotransformed by guinea pig liver slices but causes minimal cytotoxicity. Anesthesia and analgesia. 1992; 75:436–440. [PubMed: 1510266]

[47] Price RJ, Ball SE, Renwick AB, Barton PT, Beamand JA, Lake BG. Use of precision-cut rat liver slices for studies of xenobiotic metabolism and toxicity: comparison of the Krumdieck and Brendel tissue slicers. Xenobiotica. 1998; 28:361–371. [PubMed: 9604300]

[48] Leeman WR, van de Gevel IA, Rutten AA. Cytotoxicity of retinoic acid, menadione and aflatoxin B(1) in rat liver slices using Netwell inserts as a new culture system. Toxicol In Vitro. 1995; 9:291–298. [PubMed: 20650090]

[49]   Wright MC, Paine AJ. Evidence that the loss of rat liver cytochrome P450 *in vitro* is not solely associated with the use of collagenase, the loss of cell-cell contacts and/or the absence of an extracellular matrix. Biochem Pharmacol. 1992; 43:237–243. [PubMed: 1310850]

[50]   Dambach, D.M.; Andrews, B.A.; Moulin, F. New Technologies and Screening Strategies for Hepatotoxicity: Use of in Vitro Models. Toxicol. Pathol. 2004, 33, 17–26.

[51]   Brandon, E. F., Raap, C. D., Meijerman, I., Beijnen, J. H. & Schellens, J. H. An update on in vitro test methods in human hepatic drug biotransformation research: pros and cons. Toxicol. Appl. Pharmacol. 189, 233–246 (2003).

[52]   LeCluyse EL. Human hepatocyte culture systems for the in vitro evaluation of cytochrome P450 expression and regulation. European journal of pharmaceutical sciences: official journal of the European Federation for Pharmaceutical Sciences. 2001; 13:343–368. [PubMed: 11408150]

[53]   Gerets, H. H. et al. Characterization of primary human hepatocytes, HepG2 cells, and HepaRG cells at the mRNA level and CYP activity in response to inducers and their predictivity for the detection of human hepatotoxins. Cell. Biol. Toxicol. 28, 69–87 (2012).

[54]   Dunn JC, Yarmush ML, Koebe HG, Tompkins RG. Hepatocyte function and extracellular matrix geometry: long-term culture in a sandwich configuration. FASEB J. 1989; 3:174–177. [PubMed: 2914628]

[55]   Mingoia RT, Nabb DL, Yang CH, Han X. Primary culture of rat hepatocytes in 96-well plates: effects of extracellular matrix configuration on cytochrome P450 enzyme activity and inducibility, and its application in in vitro

cytotoxicity screening. Toxicol In Vitro. 2007; 21:165–173. [PubMed: 17141466]

[56] Guguen-Guillouzo C, Corlu A, Guillouzo A. Stem cell-derived hepatocytes and their use in toxicology. Toxicology. 2010; 270:3–9. [PubMed: 19815049]

[57] Guguen-Guillouzo C, Guillouzo A. General review on in vitro hepatocyte models and their applications. Methods Mol Biol. 2010; 640:1–40. [PubMed: 20645044]

[58] Lubberstedt M, Muller-Vieira U, Mayer M, Biemel KM, Knospel F, Knobeloch D, Nussler AK, Gerlach JC, Zeilinger K. HepaRG human hepatic cell line utility as a surrogate for primary human hepatocytes in drug metabolism assessment in vitro. Journal of pharmacological and toxicological methods. 2011; 63:59–68. [PubMed: 20460162]

[59] Marion MJ, Hantz O, Durantel D. The HepaRG cell line: biological properties and relevance as a tool for cell biology, drug metabolism, and virology studies. Methods Mol Biol. 2010; 640:261– 272. [PubMed: 20645056]

[60] S. Bersini, J. S. Jeon, M. Moretti, and R. D. Kamm, "In vitro models of the metastatic cascade: From local invasion to extravasation," Drug Discov. Today, vol. 19, no. 6, pp. 735–742, 2014.

[61] Godoy, P.; Hewitt, N.J.; Albrecht, U.; Andersen, M.E.; Ansari, N.; Bhattacharya, S.; Bode, J.G.; Bolleyn, J.; Borner, C.; Boettger, J.; et al. Recent advances in 2D and 3D in vitro systems using primary hepatocytes, alternative hepatocyte sources and non-parenchymal liver cells and their use in investigating mechanismsof hepatotoxicity, cell signaling and ADME. Arch. Toxicol. 2013, 87, 1315–1530.

56

[62]   Schuette, J.; Hagmeyer, B.; Holzner, F.; Kubon, M.; Werner, S.; Freudigmann, C.; Benz, K.; Boettger, J.; Gebhardt, R.; Becker, H.; et al. "Artificial micro organs"—A microfluidic device for dielectrophoretic assembly of liver sinusoids. Biomed. Microdevices 2011, 13, 493–501.

[63]   Goral VN, Hsieh YC, Petzold ON, Clark JS, Yuen PK, Faris RA (2010) Perfusion-based microfluidic device for three-dimensional dynamic primary human hepatocyte cell culture in the absence of biological or synthetic matrices or coagulants. Lab Chip 10:3380–6

[64]   Brown, L.A., Arterburn, L.M., Miller, A.P., Cowger, N.L., Hartley, S.M., Andrews, A., Silber, P.M., Li, A.P., 2003. Maintenance of liver functions in rat hepatocytes cultured as spheroids in a rotating wall vessel. In Vitro Cell. Dev. Biol. Anim. 39 (1–2), 13–20.

[65]   Schmelzer E, Mutig K, Schrade P, Bachmann S, Gerlach JC, Zeilinger K. Effect of human patient plasma ex vivo treatment on gene expression and progenitor cell activation of primary human liver cells in multi-compartment 3D perfusion bioreactors for extra-corporeal liver support. Biotechnology and bioengineering. 2009; 103:817–827. [PubMed: 19274748]

[66]   Cho, C.H., Park, J., Nagrath, D., Tilles, A.W., Berthiaume, F., Toner, M., Yarmush, M.L., 2007. Oxygen uptake rates and liver-specific functions of hepatocyte and 3T3   fibroblast co-cultures. Biotechnol. Bioeng. 97 (1), 188–199.

[67]   Nussler, A.K.; Wang, A.; Neuhaus, P.; Fischer, J.; Yuan, J.; Liu, L.; Zeilinger, K.; Gerlach, J.; Arnold, P.J.; Albrecht, W. The suitability of hepatocyte culture models to study various aspects of drug metabolism. ALTEX 2001, 18, 91–101.

[75] Chen W, Koenigs LL, Thompson SJ, Peter RM, Rettie AE, Trager WF, and Nelson SD (1998) Oxidation of acetaminophen to its toxic quinone imine and nontoxic catechol metabolites by baculovirus-expressed and purified human cytochromes P450 2E1 and 2A6. Chem Res Toxicol 11:295–301.

[76] Jaeschke H, McGill MR, Ramachandran A. Oxidant stress, mitochondria, and cell death mechanisms in drug-induced liver injury: lessons learned from acetaminophen hepatotoxicity. Drug Metab Rev 2012;44:88–106. doi: 10. 3109/03602532.2011.602688.

[77] J. A. Hinson and J. E. T. Al, "ACETAMINOPHEN-INDUCED HEPATOTOXICITY," Drug Metab. Dispos., vol. 31, no. 12, pp. 1499–1506, 2003.

[78] McGill MR, Jaeschke H. Metabolism and disposition of acetaminophen: recent advances in relation to hepatotoxicity and diagnosis. Pharm Res 2013;30: 2174–2187. doi: 10.1007/s11095-013-1007-6

[79] Luckert C, Ehlers A, Buhrke T, Seidel A, Lampen A, Hessel S (2013) Polycyclic aromatic hydrocarbons stimulate human CYP3A4 promoter activity via PXR. Toxicol Lett 222(2):180-8. doi: 10.1016/j.toxlet.2013.06.243

[80] Yun, C.-H., Shimada, T., and Guengerich, F. P. (1992) Roles of human liver cytochrome P-450 2C and 3A enzymes in the 3- hydroxylation of benzo(a)pyrene. Cancer Res. 52, 1868−1874.

[81] Bauer E, Guo Z, Ueng YF, Bell LC, Zeldin D, Guengerich FP, Oxidation of benzo[a]pyrene by recombinant human cytochrome P450 enzymes. Chemical research in toxicology 1995 Jan-Feb;8(1):136-42

[82] Gautier JC, Lecoeur S, Cosme J, Perret A, Urban P, Beaune P, Pompon D (1996) Contribution of human cytochrome P450 to benzo[a]pyrene and

benzo[a]pyrene-7,8-dihydrodiol metabolism, as predicted from heterologous expression in yeast. Pharmacogenetics. 1996 Dec;6(6):489-99

[83] Adams JD Jr, Yagi H, Levin W, Jerina DM, Stereo-selectivity and regio-selectivity in the metabolism of 7,8-dihydrobenzo[a]pyrene by cytochrome P450, epoxide hydrolase and hepatic microsomes from 3-methylcholanthrene-treated rats. Chemico-biological interactions 1995 Mar 30;95(1-2):57-77

[84] Hussein, H.S., Brasel, J.M., 2001. Toxicity, metabolism, and impact of mycotoxins on humans and animals. Toxicology 167, 101–134.

[85] Creppy, E.E., 2002. Update of survey, regulation and toxic effects of mycotoxins in Europe. Toxicol. Lett. 127, 19–28.

[86] Shen, H.M., Ong, C.N., Shi, C.Y., 1995. Involvement of reactive oxygen species in aflatoxin B1-induced cell injury in cultured rat hepatocytes. Toxicology 99, 115–123.

[87] Dohnal, V., Wu, Q., Kuca, K., 2014. Metabolism of aflatoxins: key enzymes and interindividual as well as interspecies differences. Arch. Toxicol. 88, 1635e1644.

[88] Guengerich, F. P., Shimada, T., Raney, K. D., Yun, C. H., Meyer, D. J., Ketterer, B., Harris, T. M., Groopman, J. D., and Kadlubar, F. F. (1992) Elucidation of catalytic specificities of human cytochrome P450 and glutathione S-transferase enzymes and relevance to molecular epidemiology. Environ. Health Perspect. 98, 75−80.

[89] Rawal S, Coulombe RA Jr (2011) Metabolism of aflatoxin B1 in turkey liver microsomes: the relative roles of cytochromes P450 1A5 and 3A37. Toxicol Appl Pharmacol 254(3):349–354

[90] Patterson, D. S. P., Glancy, E. M., and Roberts, B. A. (1980). The 'carry over' of aflatoxin M1 into the milk of cows fed rations containing a low concentration of aflatoxin B1. Food Cosmet. Toxicol. 18, 35–37.

[91] Neal, G.E., Eaton, D.L., Judah, D.J., Verna, A., 1998. Metabolism and toxicity of aflatoxins M1 and B1 in human- derived in vitro systems. Toxicol. Appl. Pharmacol. 151, 152–158.

[92] J. Zhang, 2015 Aflatoxin B1 and aflatoxin M1 induced cytotoxicity and DNA damage in differentiated and undifferentiated Caco-2 cells, Food and Chemical Toxicology 83 (2015) 54-60

[93] Sladek, N. E. Metabolism of oxazaphosphorines. Pharmacol. Ther., 37." 301-355, 1988.

[94] Roy, P.; Yu, L.J.; Crespi, C.L.; Waxman, D.J. (1999) Development of a substrate-activity based approach to identify the major human liver P-450 catalysts of cyclophosphamide and ifosfamide activation based on cDNA-expressed activities and liver microsomal P-450 profile. Drug Met. Disp. 1999, 27, 655-666.

[95] Clarke L and Waxman DJ (1989) Oxidative metabolism of cyclophosphamide: Identification of the hepatic monooxygenase catalysts of drug activation. Cancer Res 49:2344–2350.

[96] Chang, T. K. H., Weber, G. F., Crespi, C. L., and Waxman, D. J. (1993) Differential activation of cyclophosphamide and iphosphamide by cytochromes P-450 2B and 3A in human liver microsomes. Cancer Res. 53, 5629−5637.

[97] Huang, Z., Roy, P., and Waxman, D. J. (2000) Role of human liver microsomal CYP3A4 and CYP2B6 in catalyzing N-dechloroethylation of cyclophosphamide and ifosfamide. Biochem. Pharmacol. 59, 961−972.

[98]   IARC Working Group. Some aromatic amines, hydrazine and related substances, N-nitroso compounds and miscellaneous alkylating agents. In "IARC Monographs on the Evaluation of the Carcinogenic Risk of Chemicals to Man," Vol. 4, pp. 97–111 (1973). IARC, Lyon.

[99]   IARC Working Group. Tobacco habits other than smoking; betel-quid and areca nut chewing; and some related nitrosamines. Appendix 2. In "IARC Monographs on the Evaluation of the Carcinogenic Risk of Chemicals to Man," Vol. 38, pp. 389–394 (1985). IARC, Lyon.

[100] Kadlubar, F. F., Miller, J. A. and Miller, E. C. Hepatic microsomal N-glucuronidation and nucleic acid binding of N-hydroxy arylamines in relation to urinary bladder, carcinogenesis. Cancer Res., 37, 805–814 (1977).

[101] Kadlubar FF, Unruh LE, Flammang TJ, Sparks D, Mitchum RK, Mulder GJ, Alteration of urinary levels of the carcinogen, N-hydroxy-2-naphthylamine, and its N-glucuronide in the rat by control of urinary pH, inhibition of metabolic sulfation, and changes in biliary excretion. Chemico-biological interactions 1981 Jan;33(2-3):129-47

[102] Pacifici GM, Giuliani L, Calcaprina R, Glucuronidation of 1-naphthol in nuclear and microsomal fractions of the human intestine. Pharmacology 1986;33(2):103-9

[103] Tukey RH, Strassburg CP, Human UDP-glucuronosyltransferases: metabolism, expression, and disease. Annual review of pharmacology and toxicology 2000;40:581-616

[104] Friedman MA. Chemistry, biochemistry, and safety of acrylamide. J Agric Food Chem 2003;51:4504 – 26.

[105] IARC. Monographs on the evaluation of carcinogenic risks to humans. Vol. 60. Some industrial chemicals. Lyon: IARC; 1994. p. 389 – 433.

[106] Klaunig JE. Acrylamide carcinogenicity. J Agric Food Chem 2008;56: 5984 – 8.

[107] Manjanatha, M.G., Aidoo, A., Shelton, S.D., Bishop, M.E., McDaniel, L.P., Lyn-Cook, L.E., Doerge, D.R., 2006. Genotoxicity of acrylamide and its metabolite glycidamide administered in drinking water to male and female Big Blue mice. Environ. Mol. Mutagen. 47, 6–17.

[108] Settels E, Bernauer U, Palavinskas R, Klaffke HS, Gundert-Remy U, Appel KE. Human CYP2E1 mediates the formation of glycidamide from acrylamide. Arch Toxicol 2008;82:717 – 27

[109] Kurebayashi H, Ohno Y. Metabolism of acrylamide to glycidamide and their cytotoxicity in isolated rat hepatocytes: protective effects of GSH precursors. Arch Toxicol 2006;80:820– 8.

[110] Koyama N, Sakamoto H, Sakuraba M, Koizumi T, Takashima Y,Hayashi M, Matsufuji H, Yamagata K, Masuda S, Kinae N, Honma M (2006) Genotoxicity of acrylamide and glycidamide in human lymphoblastoid TK6 cells. Mutat Res 603:151–158

[111] Boettcher MI, Bolt HM, Drexler H, Angerer J. Excretion of mercapturic acids of acrylamide and glycidamide in human urine after single oral administration of deuterium-labelled acrylamide. Arch Toxicol 2006;80:55 – 61

[112] Fuhr U, Boettcher MI, Kinzig-Schippers M, et al. Toxicokinetics of acrylamide in humans after ingestion of a defined dose in a test meal to improve risk assessment for acrylamide carcinogenicity. Cancer Epidemiol Biomarkers Prev 2006;15:266 – 71.

[113] Smylie, M. G., Wong, R., Mihalcioiu, C., Lee, C., and Pouliot, J. F., A phase II, open label, monotherapy study of liposomal doxorubicin in patients with metastatic malignant melanoma. Invest. New Drugs, 25, 155-159 (2007).

[114] G. Minotti, R. Ronchi, E. Salvatorelli, P. Menna, G. Cairo, Cancer Res. 61 (2001) 8422-8428.

[115] G.X. Wang, Y.X. Wang, X.B. Zhou, M. Korth, Eur. J. Pharmacol. 423 (2001) 99-107.

[116] D.J. Stewart, D. Grewaal, R.M. Green, N. Mikhael, R. Goel, V.A. Montpetit, M.D. Redmond, Anticancer Res. 13 (1993) 1945-1952.

[117] Olson RD, Mushlin PS, Brenner DE, Fleischer S, Cusack BJ, Chang BK, Boucek RJ., Jr Doxorubicin cardiotoxicity may be caused by its metabolite, doxorubicinol. Proc Natl Acad Sci U S A. 1988 May;85(10):3585–3589

[118] Delclos,K.B., El-Bayoumy,K., Hecht.S.S., Walker.R.P. and Kadlubar.F.F. (1988) Metabolism of the carcinogen [3H]6-nitrochrysene in the preweanling mouse: identification of 6-aminochrysene-1,2-dihydrodiol as the probable proximate carcinogenic metabolite.

[119] Delclos,K.B., Miller.D.W., Lay Jr,J.O., Casciano.D.A., Walker.R.P., Fu,P.P. and Kadlubar.F.F. (1987) Identification of C8-modified deoxyinosine and N2- and C8-modified deoxyguanosine as major products of the in vitro reaction of M-hydroxy-6-aminochrysene with DNA and the formation of these adducts in isolated rat hepatocytes treated with 6-nitrochrysene. Carcinogenesis, 8, 1703-1709.

[120] Kadlubar.F.F. and Hammons.G.J. (1987) Role of cytochrome P-450 in the metabolism of chemical carcinogens. In Guengerich.F.P. (ed.), Mammalian Cytochromes P-450. Vol. 2, CRC Press, Boca Raton, FL, pp. 81 -130.

[121] Shimada,T., Iwasaki,M., Martin,M.V. and Guengerich.F.P. (1989) Human liver microsomal cytochrome P-450 enzymes involved in the bioactivation of procarcinogens detected by umu gene response in Salmonella typhimurium TA1535/pSK1002. Cancer Res., 49, 3218-3228.

[122] Yamazaki, H., Mimura, M., Oda, Y., Inui, Y., Shiraga, T., Iwasaki, K, Guengerich, F. P., and Shimada, T. (1993) Roles of different forms of cytochrome P450 in the activation of the promutagen 6- aminochrysene to genotoxic metabolites in human liver microsomes. Carcinogenesis 14, 1271−1278.

[123] Yamazaki, H., Mimura, M., Oda, Y., Gonzalez, F. J., El-Bayoumy, K., Chae, H. Y., Guengerich, F. P., and Shimada, T. (1994) Activation of trans-1,2-dihydro-1,2-dihydroxy-6-aminochrysene to genotoxic metabolites by rat and human cytochromes P450. Carcinogenesis 15, 465−470.

[124] Gilchrest BA, Oral methoxsalen photochemotherapy of mycosis fungoides. Cancer. 1976 Aug;38(2):683-9.

[125] Deeni YY, Ibbotson SH, Woods JA, Wolf CR, Smith G. Cytochrome P450 CYP1B1 interacts with 8-methoxypsoralen (8-MOP) and influences psoralen-ultraviolet A (PUVA) sensitivity. PLoS One. 8(9):e75494. doi: 10.1371/journal.pone.0075494

[126] Agency for Toxic Substances and Disease Registry, U.S. Public Health Service "Toxicological Profile For Nitrophenols".. July 1992.

[127] Wongwiwat T, Validation of 4-nitrophenol as an in vitro substrate probe for human liver CYP2E1 using cDNA expression and microsomal kinetic technique, Biochemical Pharacology, 1993

[128] McCoy GD and Koop DR, Biochemical and immunochemical evidence for the inducible of an ethanol-inducible cytochrome P-450 isozyme in male syrian golden hamsters. Biochem Pharmaco137: 1563-1568, 1988.

[129] Sinclair JF, Wood SG, Smith EL, Sinclair PR and Koop DR, Comparison of the form(s) of cytochrome P-450 induced by ethanol and glutethimide in cultured chick hepatocytes. Biochem Pharmacol 38: 657-664, 1989.

[130] Zerilli A, Ratanasavanh D, Lucas D, Goasduff T, Dréano Y, Menard C, Picart D, Berthou F (1997) Both cytochromes P450 2E1 and 3A are involved in the O-hydroxylation of p-nitrophenol, a catalytic activity known to be specific for P450 2E1. Chem Res Toxicol. 1997 Oct;10(10):1205-12. doi: 10.1021/tx970048z

[131] D. Bratosin, L. Mitrofan, C. Palii, J. Estaquier, and J. Montreuil, "Novel fluorescence assay using calcein-AM for the determination of human erythrocyte viability and aging," Cytom. Part A, vol. 66, no. 1, pp. 78–84, 2005.

[132] Crouch, S.P. et al. (1993) The use of ATP bioluminescence as a measure of cell proliferation and cytotoxicity. J. Immunol. Methods 160, 81–8.

[133] Kangas, L., Gronroos, M. and Nieminen, A.L. (1984) Bioluminescence of cellular ATP: A new method for evaluating cytotoxic agents in vitro. *Med. Biol.* 62, 338–43.

[134] Lundin, A. *et al.* (1986) Estimation of biomass in growing cell lines by adenosine triphosphate assay. *Methods Enzymol.* 133, 27–42.

[135] Lee MY, ed. (2017) Microarray Bioprinting Technology: Fundamentals and Practices. Springer

[136] Lee MY, Dordick JS, Clark DS (2010) Metabolic enzyme microarray coupled with miniaturized cell-culture array technology for high-throughput toxicity

screening. Methods Mol Biol. 632:2212-37. doi: 10.1007/978-1-60761-663-4_14

[137] Sui Y, Wu Z (2007) Alternative statistical parameter for high-throughput screening assay quality assessment. J Biomol Screen 12(2):229-34. doi: 10.1177/1087057106296498 Sui Y, Wu Z (2007) Alternative statistical parameter for high-throughput screening assay quality assessment. J Biomol Screen 12(2):229-34. doi: 10.1177/1087057106296498

[138] Mironov SL, Ivannikov MV, Johansson M (2005) [Ca2+]i signaling between mitochondria and endoplasmic reticulum in neurons is regulated by microtubules. From mitochondrial permeability transition pore to Ca2+-induced Ca2+ release. J Biol Chem 280(1):715-721. doi: 10.1074/jbc.M409819200

[139] Joshi P, Datar A, Yu KN, Kang SY, Lee MY (2018) High-content imaging assays on a miniaturized 3D cell culture platform. Toxicol In Vitro 50:147-159. doi: 10.1016/j.tiv.2018.02.014

[140] Riss TL, Moravec RA, Niles AL, Duellman S, Benink HA, Worzella TJ and Minor L. (2013). Cell viability assays. in Assay Guidance Manual [internet] (G. S. Sittampalam, N. Gal-Edd, M. Arkin,

[141] Gundert-Remy U, Bernauer U, Blömeke B, Döring B, Fabian E, Goebel C, Hessel S, Jäckh C, Lampen A, Oesch F, Petzinger E, Völkel W, Roos PH (2014) Extrahepatic metabolism at the body's internal-external interfaces. Drug Metab Rev 46(3):291-324. doi: 10.3109/03602532.2014.900565

[142] Raccor BS, Claessens AJ, Dinh JC, Park JR, Hawkins DS, Thomas SS, Makar KW, McCune JS, Totah RA (2012) Potential contribution of cytochrome P450

2B6 to hepatic 4-hydroxycyclophosphamide formation in vitro and in vivo. Drug Metab Dispos 40(1):54-63. doi: 10.1124/dmd.111.039347

[143] Yang L, Yan C, Zhang F, Jiang B, Gao S, Liang Y, Huang L, Chen W (2018) Effects of ketoconazole on cyclophosphamide metabolism: evaluation of CYP3A4 inhibition effect using the in vitro and in vivo models. Exp Anim 67(1):71-82. doi: 10.1538/expanim.17-0048

[144] Yu KN, Nadanaciva S, Rana P, Lee DW, Ku B, Roth AD, Dordick JS, Will Y, Lee MY (2017) Prediction of metabolism-induced hepatotoxicity on three-dimensional hepatic cell culture and enzyme microarrays. Arch Toxicol 92(3):1295-1310.   doi: 10.1007/s00204-017-2126-3.